*Journal of Geophysical Research: Planets*

Supporting Information for

# Survey of Galileo Plasma Observations in Jupiter's Plasma Sheet

Fran Bagenal[1], Robert J. Wilson[1], Scott Siler[1], William R. Paterson[2], William S. Kurth[3]

1) Laboratory of Atmospheric and Space Physics, University of Colorado Boulder, CO, USA
2) Goddard Space Flight Center
3) University of Iowa

## Contents of this file



## Introduction

This supporting information is a single document that describes the difficulties in analyzing the Galileo PLS data set. It contains information on calibrations used, how the individual PDS level 3 data records were combined in to spins, the method of analysis used in the main article, and other information (including errata) useful for any future analysis, which had not previously been collated in a single document.

# Analysis of Galileo PLS Ion Data: Why it is so difficult?

**Table of Contents**

## 1. Introduction – Merging Data Products to Make a Spectrum

Galileo PLS data are hard to interpret for four reasons:

1. *A misfortune of nature:* PLS is an energy-per-charge instrument, and several ion species at Jupiter share the same mass-per-charge so cannot be differentiated, i.e. the two dominant species $S^{++}$ and $O^{+}$ both have a mass-per-charge of 16 amu/e.
2. *An instrumental issue:* The Geometric Factor of the PLS instrument is smaller than needed to measure low plasma fluxes in the outer jovian magnetosphere.
3. *A mission misfortune:* With Galileo's main antenna out of operation, the data rate for all instruments were decimated which forced many hard choices on how the instrument would be operated.
4. *Miscommunications:* There are slip-ups in publications/PDS documents about pointing and calibrations that had to be identified and corrected.

PLS measures ions, electrons and has a mass spectrometer mode. PLS is an electrostatic analyzer that imposes a voltage between plates, stepped across a range of voltages, to separate the particles by energy per charge. Throughout this document these voltage steps are referred to as energy steps, energy/charge steps, energy per charge or E/q intervals.

This work concentrates on the ion data, which comprise nearly 50% of the returned data (the mass spectrometer mode was rarely used, and the rest of the data are split between electrons and ions). However, the raw data from PLS merges these three modes, each consisting of counts per accumulation period where the resulting number is compressed with a 16 bit -> 8 bit look up table (resulting in only 256 unique values being returned). While this 2-byte to 1-byte compression is typical for spacecraft, 33 of those 256 unique values (~1/8th) were never used, meaning the data were over-compressed. There were 117,787,477 one-byte data objects returned from PLS from 1995-2003, a total of 112 megabytes over 9 years. The originally planned mission would have returned much more data and the low total data return is directly related to the failed antenna. Moreover, because of the low geometric factor of the instrument 91,923,579 of the returned data objects (78%) had a zero value, and 90% of the data objects have 8 or less counts per accumulation. There are also periods of higher counts that are due to periods where high backgrounds swamp the data. As a result, we are restricted to times when there are enough counts above background, which tends to be closer to Jupiter (<30 $R_J$).

PLS Level 3 data are stored at the Planetary Data System (https://pds.nasa.gov/) and are stored in volume GO-J-PLS-3-RDR-FULLRES-V1.0 (called PDS-doc for short). Each record states: the time assigned to the singular measurement; the value of counts per second; whether the number is for the mass spectrometer, the electron or ion sensor (including

the anode number); the energy/charge step number; the mass step (only non-zero for mass spectrometer records); the accumulation time (thus allowing counts/sec to be converted to counts/accumulation); plus a sample number and sector ID to put that record in context within the spacecraft 'spin' period.

Due to the antenna malfunction, it was impossible to return to Earth the data corresponding to all energy/charge steps in a sweep (comprising 64 steps numbered from 0 to 63, low to high eV/q). This required severe compromises, resulting in a subset of energies per sweep for each spin being returned, as described below.

The PLS data were returned in four different modes with four different accumulations times (known as ACCUM_TIME in PDS records). The four descriptions are easiest to understand in figure form, as shown in *Figure 1*. The accumulation times are all multiples of 1/60th second due to the resolution of the spacecraft clock sub-ticks.

**Mode 1: ACCUM_TIME =0.1667 seconds = 10/60$^{th}$ s – 1 flavor**
This mode returns just the lowest 16 consecutive steps of the full 64 steps [steps 0-15], and was intended for use with electron data to help identify spacecraft potential. The instrument is built such that the ion and electron detectors sample the same energy steps, and for ions the lowest 16 energies have essentially no plasma signal in the jovian magnetosphere. This mode is ignored for the forward fitting method of ion analysis. There is just one type of 0.1667 ACCUM_TIME record, hence just 1 flavor.

**Mode 2: ACCUM_TIME =0.5000 seconds = 30/60$^{th}$ s – 2 flavors**
This mode only returns every 4th energy step, but in two flavors, high and low. The high flavor covers every 4th energy step from 39 to 63 inclusive, while the low flavor covers every 4th energy step from 11 to 35 inclusive. By combining a low flavor spin with a high flavor spin you can get every 4th energy step from 11 to 63. The three steps between every 4th step, and steps 0 to 10, are never returned.

**Mode 3: ACCUM_TIME =0.2667 seconds = 16/60$^{th}$ s – 2 flavors**
This mode only returns every 3rd energy step, but in two flavors, high and low. The high flavor covers every 3rd energy step from 42 to 63 inclusive, while the low flavor covers every 3rd energy step from 18 to 39 inclusive. By combining a low flavor spin with a high flavor spin you can get every 3rd energy step from 18 to 63. The two steps between every 3rd step, and steps 0 to 17, are never returned.

**Mode 4: ACCUM_TIME =0.1500 seconds = 9/60$^{th}$ s – 4 flavors**
This mode only returns every 4th energy step, but in four flavors that interleave each other. These are every 4$^{th}$ energy step from 12 to 60 inclusive, every 4$^{th}$ energy step from 13 to 61 inclusive, every 4$^{th}$ energy step from 14 to 62 inclusive and every 4$^{th}$ energy step from 15 to 63 inclusive. By combining a spin from each of the 4 flavors you get every energy step from 12 to 63 with no gaps. Only the low energy steps 0-11 are never returned.

Clearly, accumulation time (known as ACCUM_TIME in PDS records) of 0.1500s is the highest resolution. It requires 4 consecutive spacecraft spins (one in each flavor) to build up the full resolution, assuming the underlying plasma population does not change during that interval. This is an issue when the plasma conditions likely change within that time (for instance, during fly-bys of moons).

Temporal changes in plasma conditions can also be an issue for the lower data products. The low flavor ACCUM_TIME = 0.5s spin may be taken 15 minutes after the high flavor. As before one needs to assume the underlying plasma conditions have not changed during that interval, and that both flavors share a common background count value per anode.

It should also be noted that the odd anodes are in different data packets to the even anodes. This was done deliberately as a form of redundancy since the odd anodes have hemispheric voltages supplied by a different generator to the even anodes, just in case there was a failure on one set of voltages there would still be data from the other. This also has the consequence that the energy tables used for the 64 energy steps are slightly different between the odd and even anodes. Likewise, the calibrations for geometric factor and efficiencies are split between the odd and even anodes. This information can be found in the CALIB directory of PDS-doc. The Geometric Factor and efficiency are combined to one number, and are given as a scalar for each anode (i.e. not dependent on energy nor ion species).

The fact that odd and even anodes come down in different packets complicates items further. It was decided that pointing information was more important than absolute time, so that each record contains a spin-phase by way of the SECTOR_ID object (a 1-byte representation of 0-360 degrees with values of 0-255, which rolls over so that there are occasional values of 256=0, 257 = 1, etc.). The time stamp on the packet is then the time that the packet reached Galileo's onboard data storage system, not the start time of the data. Various delays within the onboard processing chain meant that the odd and even anode packets rarely arrived at the storage area at the same time, and were often several seconds apart. This happens inconsistently. Sometimes the odd packet arrived first, sometimes the even. This makes merging the odd and even packets in to one array of all anodes for a spin more complicated.

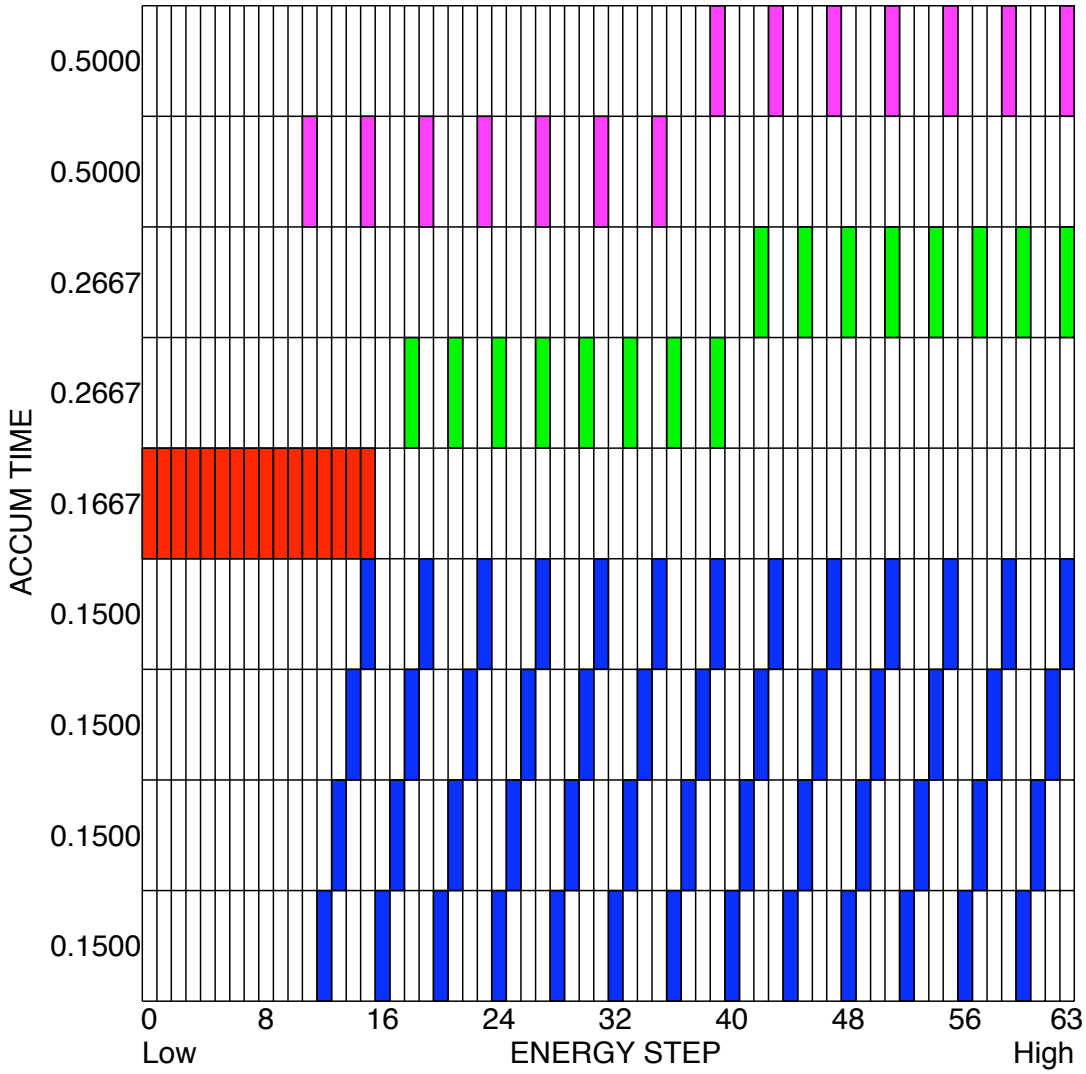


*Figure 1: The four different accumulation times of PLS data and their different flavors. Modes 1, 2, 3 and 4 are shown in red, magenta, green and blue respectively.*

For Mode 4 (ACCUM_TIME = 0.1500s) and given a Galileo spin period was approximately 19 seconds, if the packet times are within 10 seconds of each other they are likely from the same spin, and definitely from the same spin if within 5 seconds. For modes 3 and 2 (ACCUM_TIMEs of 0.2667s and 0.5000s) the records only return odd or even anodes for a given spin, with a later spin (not necessarily the next spin) returning the other. It should also be noted that there are occasions when either the odds or evens are missing.

Next we consider the complications of merging the different flavors of each data type. Not every spin record of data starts immediately after the previous one. Nor is it the case that each spin record starts at the same spin phase. However the record will always start on a $1/8^{th}$ spin boundary. Mode 4 (ACCUM_TIME = 0.1500s) records may start a

sweep of every 4$^{th}$ energy step at a spin phase of 0 degrees. If the record completes its sweep before the spin phase has reached 45 degrees there is a wait period. Upon hitting a spin phase of 45 degrees, the record starts the next sweep. The same happens again at 90, 135, 180, 225, 270, and 315 degrees. Note that the records could start the spin of 8 sweeps at a spin phase of any multiple of 45 degrees.

By comparison ACCUM_TIME of 0.2667 or 0.5000 have spin records that do 4 sweeps per spin starting at spin phases of 0, 90, 180 or 270 degrees. This is because each sweep takes enough time that it has not finished within 1/8th of a spin, so it finishes and then waits for the next 1/8th boundary (i.e. to reach the quarter spin boundary) before starting again.

In addition, there can be pauses of 3/8$^{th}$ of a spin between data records. Furthermore, Mode 1 (ACCUMU_TIME of 0.1667) data tend to occur 3 consecutive records at a time, each taking just over 2/8ths of a spin each, thus having a wait for the 3rd eighth marker point before starting the next record. This means the group of 3 records takes 9/8$^{th}$ of a spin.

All these factors result in 'spin' packets starting at any one of 8 different spin phases, an extra complication to include when merging four flavors of spins together. The net effect is best explained by example. For example, data could be returned as follows:

1 spin (8 sweeps) of ACCUM_TIME = 0.1500s for every 4th energy step from 13 to 61
1 spin (8 sweeps) of ACCUM_TIME = 0.1500s for every 4th energy step from 15 to 63
1 spin for mass spectroscopy - ignored
1 spin (8 sweeps) of ACCUM_TIME = 0.1500s for every 4th energy step from 12 to 60
1 spin (8 sweeps) of ACCUM_TIME = 0.1500s for every 4th energy step from 14 to 62
Pause for 3/8th of a spin - ignored
1 spin for mass spectroscopy - ignored
1 spin (8 sweeps) of ACCUM_TIME = 0.1500s for every 4th energy step from 13 to 61
1 spin (8 sweeps) of ACCUM_TIME = 0.1500s for every 4th energy step from 15 to 63
Pause for 3/8th of a spin - ignored
1 spin for mass spectroscopy - ignored
1 spin (8 sweeps) of ACCUM_TIME = 0.1500s for every 4th energy step from 12 to 60
1 spin (8 sweeps) of ACCUM_TIME = 0.1500s for every 4th energy step from 14 to 62
1 sweep of ACCUM_TIME = 0.1667 s (taking 3/8th of a spin)
1 sweep of ACCUM_TIME = 0.1667 s (taking 3/8th of a spin)
1 sweep of ACCUM_TIME = 0.1667 s (taking 3/8th of a spin)

Visually, merging this sequence we get Figure 2 where the x-axis is number of sectors (each 1/8$^{th}$ of a spin). A total of 13 Galileo spins were required to build up two merged records of energy steps 12 to 63. The first required 5 spins, where each of the four flavors of Mode 4 (ACCUM_TIME = 0.1500s) started at the same spin-phase. However the second grouping of 4 ACCUM_TIME = 0.1500s records starts at a different spin-

phase to the first merged spin, and the latter two spins start at a different spin-phase than the first two for that second merged spin. This can be dealt with in code, but the code has to account for each 'record spin' starting at a different spin-phase.

In Figure 3 we show the resulting spectra. The top panel shows the raw spectrograms of PLS ion data from anode 3, where the x-axis is hour:minute of 1995-12-07. The width of each polygon is true to the accumulation period, and you can see the 8 values per spin before it changes to the next flavor of data. The co-rotational flow shows up in red in just 1 of the 8 sectors per spin and clearly moves about within the groupings of 8 as the start spin phase of each data-spin starts.

The bottom panel shows what it looks like if you merge the 4 flavors to get one 'whole' packet, what we call a merged-spin. This time the width of each column is no longer the true accumulation time but is $1/8^{th}$ of the period it took to collect all 4 spins (not necessarily consecutive) of ACCUM_TIME – 0.1500s data, and that period may be 4 spins, 5 spins, $5 + 3/8^{th}$ spins, etc., and is purely for visual convenience to align with the separate spins on the top panel. Note that there is no guarantee that all 4 flavors are available to merge to a record. Missing 1 of the 4 is pretty common.

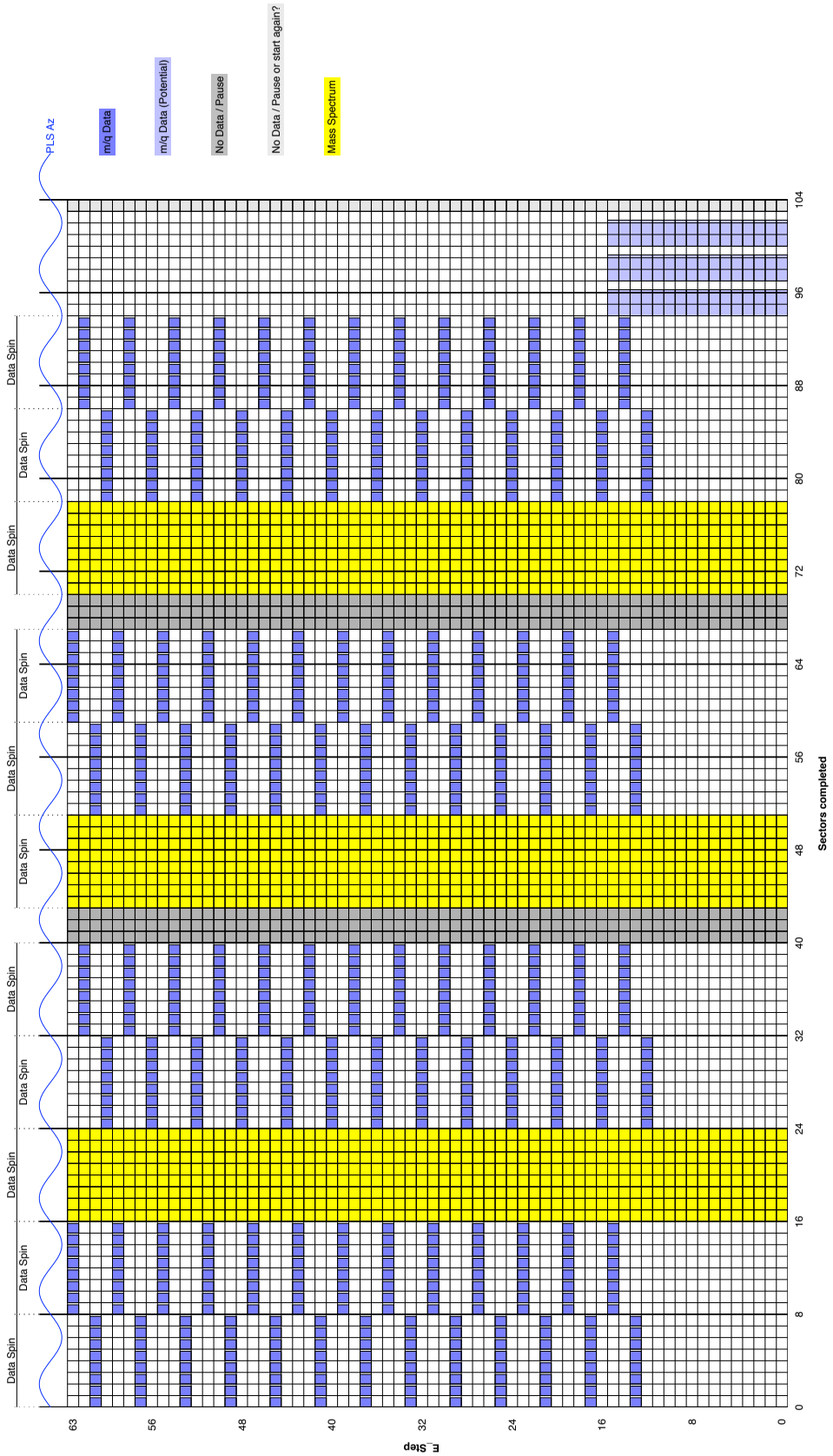


*Figure 2: Example of how PLS takes high rate data.*

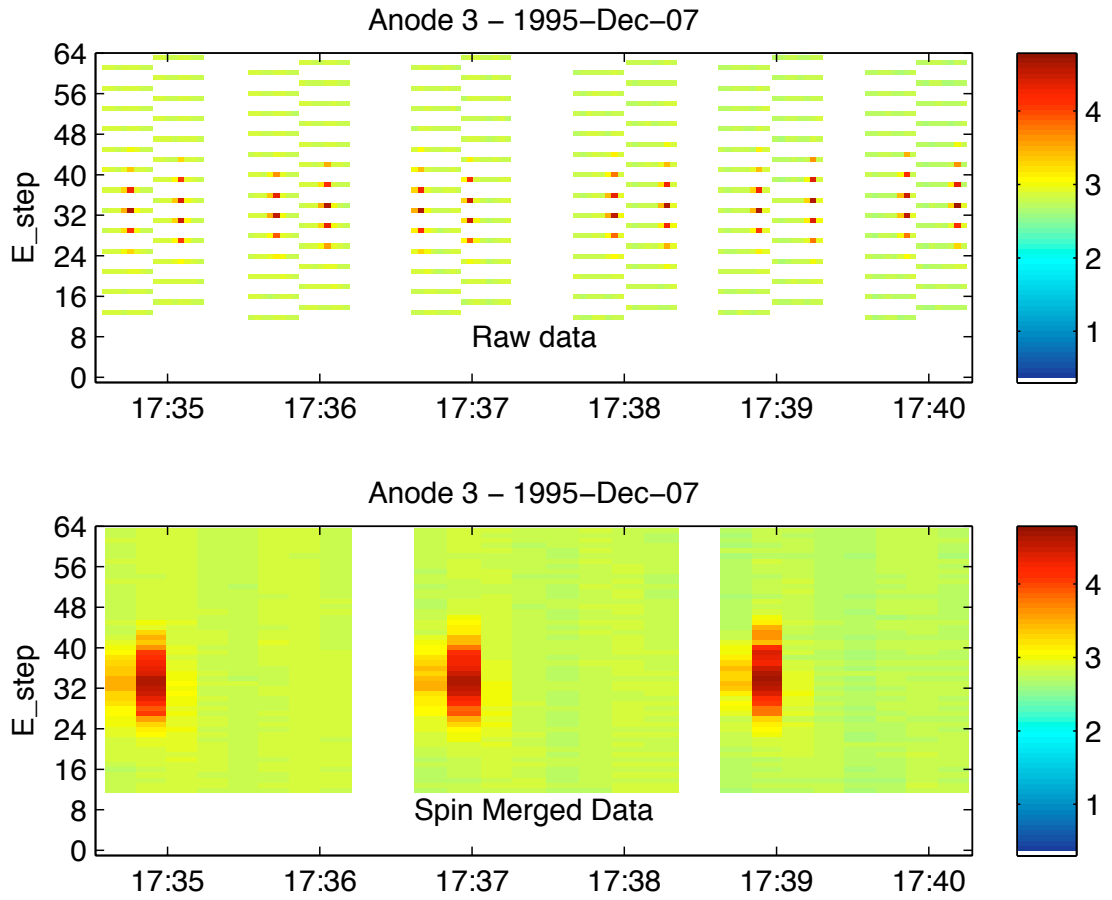


*Figure 3: Example of Mode 4 (ACCUM_TIME = 0.1500s) raw spins (top) and 'merged-spins' (bottom). Colorbar is Log10(Counts/Accumulation), x-axis is HH:MM of 1995-Dec-07.*

This example (Figure 3 above) shows that the co-rotating ion beam measured by PLS is often only seen in one sweep during the spin, perhaps with some counts in a neighboring sweep. Likewise it is common that the co-rotation ion beam is only seen strongly in one anode and a little bit in its neighboring anodes. However, many times the beam enters an end anode (anode 1 or anode 7). Therefore, there is only one neighboring anode. These effects make it harder to pin down directional information about the plasma flow as there are few unique anode/sweeps that measure the corotating beam.

To show the time spread of the individual flavor and odd/even anode spins, Figure 4 shows examples of raw spectrograms for anodes 1 and 2 for ACCUM_TIMEs of 0.2667s (figure 4a) and 0.5000s (figures 4b), where the polygons shown are to their true accumulation times. It can take 8 to 15 minutes to return one of each flavor for both odd and even anodes.

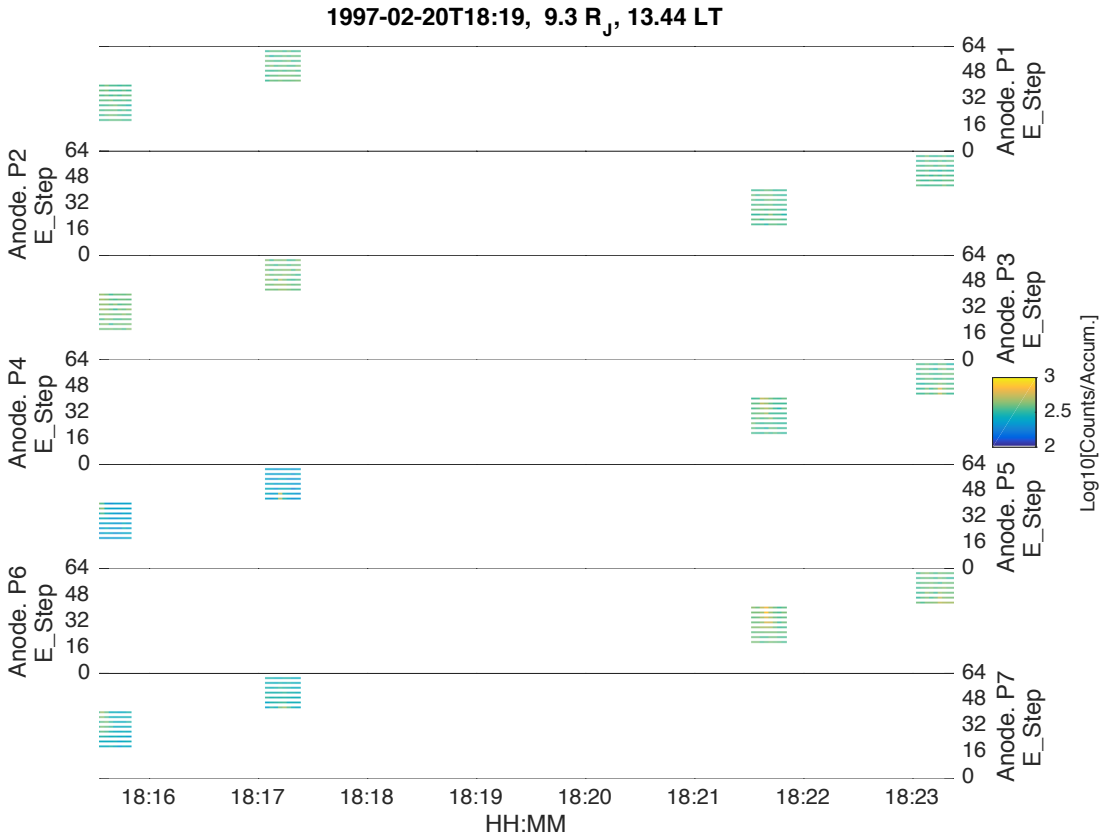


*Figure 4a: Example of how medium rate spins (ACCUM_TIME = 0.2667 s) are returned and the gaps in time between data-returning spins. Anode = Detector, Colorbar is Log10(Counts/Accumulation), x-axis is HH:MM of 1997-Feb-20. Please zoom in to this PDF to see the finer structure within the blocks of color, plotted to their true accumulation times. Figure 4b on the next page shows two more examples for low rate spins.*

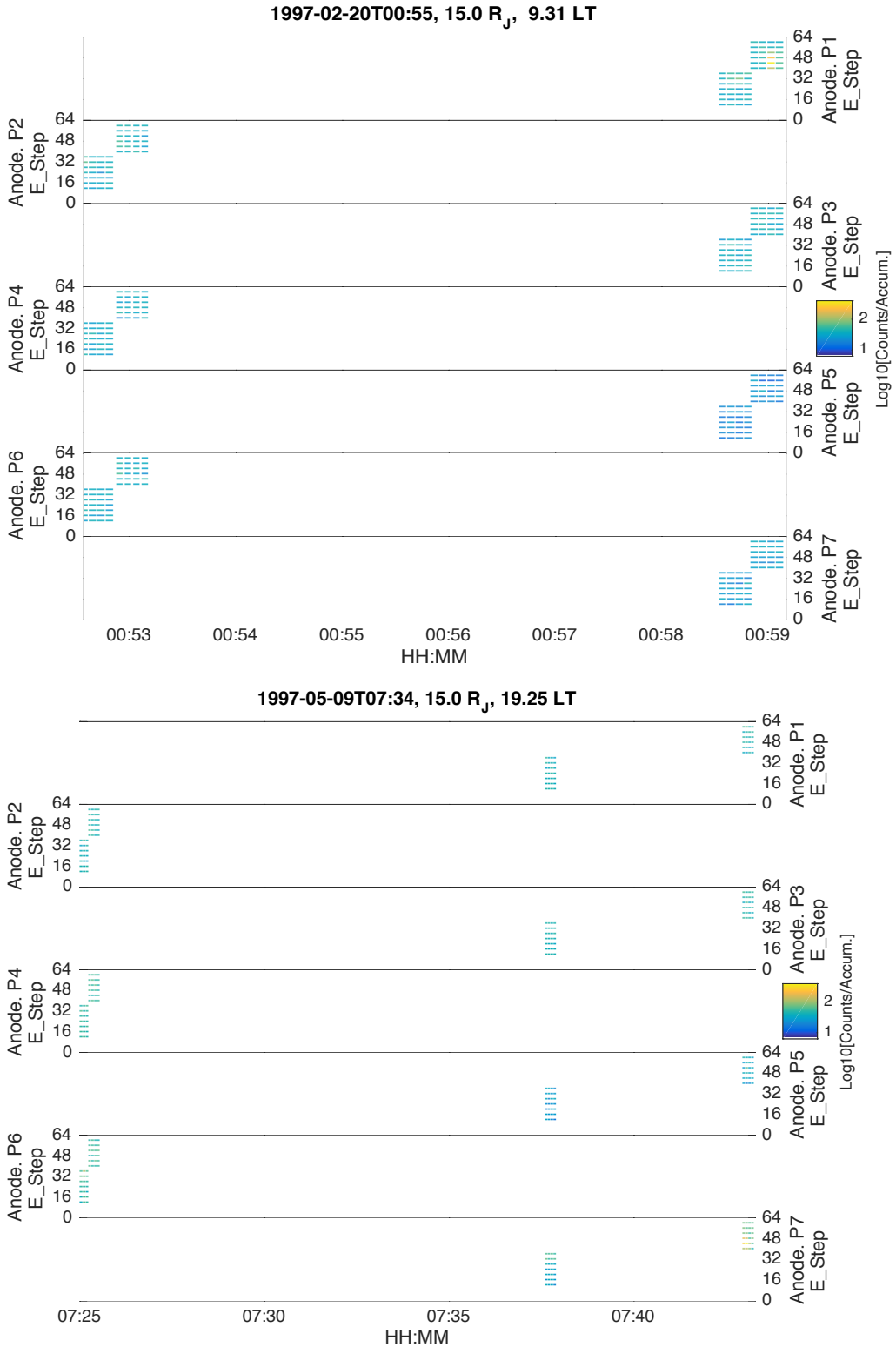


*Figure 4b – Examples of how low rate spins (ACCUM_TIME = 0.5 s) are returned and the gaps in time between data-returning spins. Anode = Detector, Colorbar is Log10(Counts/Accumulation), x-axis is HH:MM of 1997-Feb-20 (top) or 1997-05-09 (bottom).*

## 2. Spatial Distribution of Data of Different Modes

The data are decimated from the full 64-energy/charge step sweeps originally planned prior to the antenna malfunction. For this study we use the ion data only (not mass-spectrometer data), and only Modes 4, 3, and 2 (ACCUM_TIMEs of 0.1500, 0.2667 and 0.5000 seconds), otherwise known as high, medium, and low resolutions respectively. The vast majority of the data is in the lowest resolution. The highest resolution data are predominantly only taken during moon encounters, within a very restricted radial distances from Jupiter. All PLS data from the PDS volume were examined, rearranged into 9,368 'merged-spin' records. Data that did not measure significant counts were removed. This was predominantly at distances greater than 30 $R_J$ - eliminating nearly two thirds of the records. Likewise, data within 10 moon radii of a Galilean moon were removed as the plasma environment by the moons can change much faster than the cadence of merged-spins.

Of the 3,395 records that were left, Figure 5 shows where those 1,902 intervals within 30 $R_J$ were located. These were the spectra to which we applied the Forward Modeling (FM). The distribution of data is shown on an equatorial plane since Galileo's trajectory over the mission was predominantly near the equator. Most of the data occurs at the lowest resolution, and the high resolution data were taken mostly near the moon encounters. The 1,493 records outside 30 $R_J$ could be fit mathematically, but with difficulty given low count rates. Most of the data outside 30 $R_J$ gave uncertainties on the fit parameters of 100-300%. This study concentrates on data within 30 $R_J$.

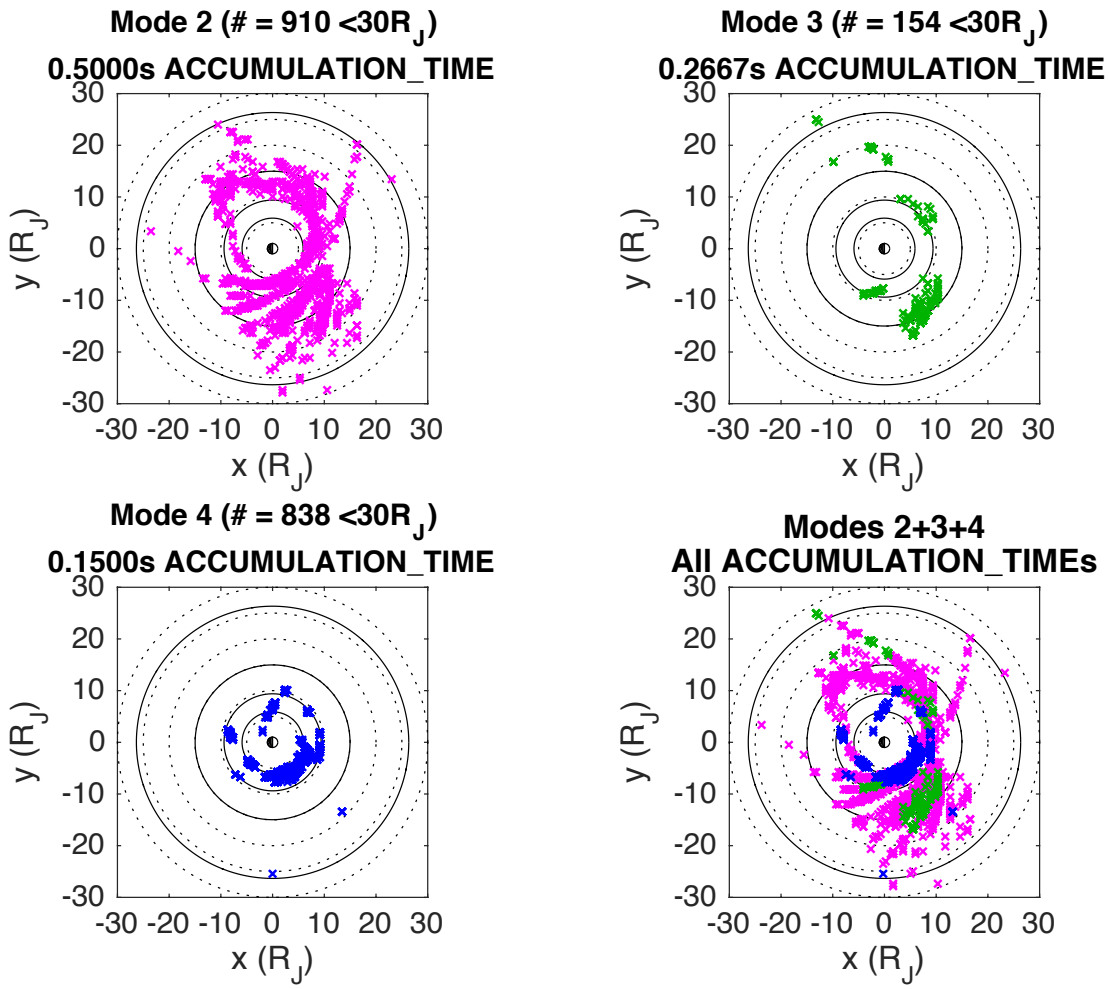


*Figure 5: Distribution of different PLS modes, High, Medium and Low Resolution for the 1,902 merged-spin records within 30 $R_J$ considered in this study. The Sun is at +x and solid circles show the orbits of the four Galilean moons. The number of merged-spins of each type is shown in the titles. Mode 2, 3, and 4 are shown in magenta, green and blue respectively.*

## 3. Background Calculation

Normally, a background value per anode per sweep is calculated to derive plasma parameters from the data. But with PLS data this is not always possible. A common technique is to use an average of the highest few energy/charge steps as a measurement of background, as the bulk plasma population is far below that. However, for the lower and medium resolution data, the lower half of the energy samples are returned in a different spin at a later time and there is no good value to use for background. Consequently, the data were put into merged-spins (see bottom panel of Figure 3) and the background used was simply the value of the highest step (step 63).

The assumption is that the background did not alter during the 4 flavor spins of high resolution or the 2 flavor spins of low/mid resolution data.

This is a reasonable approximation, but fails when flying through a moon's wake as the plasma environment is simply changing too quickly. We therefore excluded moon fly-bys (defined as Galileo within 10 $R_{moon}$ of the moon) from this study.

## 4. Uncertainty of Velocity Direction Based on Timing of Sweeps

The majority of the data are in low resolution Mode 2 (ACCUM_TIME = 0.5000s), with 4 azimuthal sweeps through energy per spin. This means that each energy/charge step is only measured 4 times per spin (exactly 90 degrees apart). The data are not taken at the moment when the anode is pointed into the plasma flow. The start of a sweep is related to sector ID, and is essentially aligned with ECL-50's +Z pole vector ('north') (rather then, for instance, Jupiter's spin equator, where the plasma is corotating).

To walk through this issue, let us assume as a thought experiment that Jupiter's magnetic pole is aligned with the spin axis, and sector_ID = 0 is also aligned with the spin axis, which we will call north, and anti-parallel to the spin direction south. At the same time, assume that the Galileo spacecraft has its spin axis aligned with the equator. The main co-rotation ion beam is incident from the direction pointing upstream along Jupiter's spin equator, which we will call west (this puts the ion flow in the east direction) and centered at an energy/charge of ~2 keV, at step 43. For low resolution data each sweep takes every 4th energy step to measure 7 steps of the high energy flavor mode, in order: 39, 43, 47, 51, 55, 59, 63.

Assuming a 20-second spin for the spacecraft (for mathematical simplicity, the actual spin period is closer to 19s), every 0.5s accumulation period covers 6.5 degrees, so step 43 is measured from 6.5 through 13 degrees offset from each compass point. Given the narrowness of the ion bean, only the one-sided offset from the west looking direction will measure any counts.

Under such conditions, the instrument only measures the important ~2keV energy beam once per spin, when looking at the corotation direction off-center from its true incident direction. Analysis of the data will identify a flow with a component that is also off-center (e.g. inward or outward, up or down). In doing a forward fit to the data, the code does the best it can with the data it has, but without multiple samples of the ion beam, looking on both sides of the ion beam, the non-dominant radial (r) and poloidal ($\theta$) velocity components are poorly constrained. The situation is worse when the real peak energy of the ion beam is not on a measured step, e.g. if the peak energy would have been measured at step 45 but we only sample step 43 and 47 then it is likely we will underestimate the true density.

The same principle as illustrated in the above thought experiment applies in more realistic situations where none of the spin poles are aligned so neatly. Given Galileo remains in much the same orientation for most of its life at Jupiter (pointing at Earth), it often only measures the main ion beam in one azimuth sweep, providing non-zero $V_r$ and $V_\theta$ components that potentially have a local-time dependence based on nothing more than geometry of the different spin poles at different locations and restricted sampling of data. However, given the large uncertainties also found in the $V_r$ and $V_\theta$ components from our modeling compared to their absolute (small relative to $V_\varphi$) values, it is probably safe to assume that $V_r$ and $V_\theta$ are always approximately zero to within our ability to measure these non-azimuthal flows with Galileo PLS data.

## 5. Galileo Spin Direction and PLS Anode Placement

The Galileo PLS instrument paper [Frank et al. 1992] has a figure from 1992, shown below on the left side of Figure 6. It shows end anodes 1 and 7 leading middle anode 4 during a spin. It was subsequently realized that the middle anode leads the end anodes, and this was changed in a figure from Paterson [2009] final report on NASA Grant NNG05GJ23G, where the figure is shown below on the right. After further analysis, we believe anode 4 leads the other anodes; the spin direction needs to be changed from shown in the right of Figure 6. We are not sure of the origin of this confusion but suspect that between design and arrival at Jupiter the direction of spin was changed.

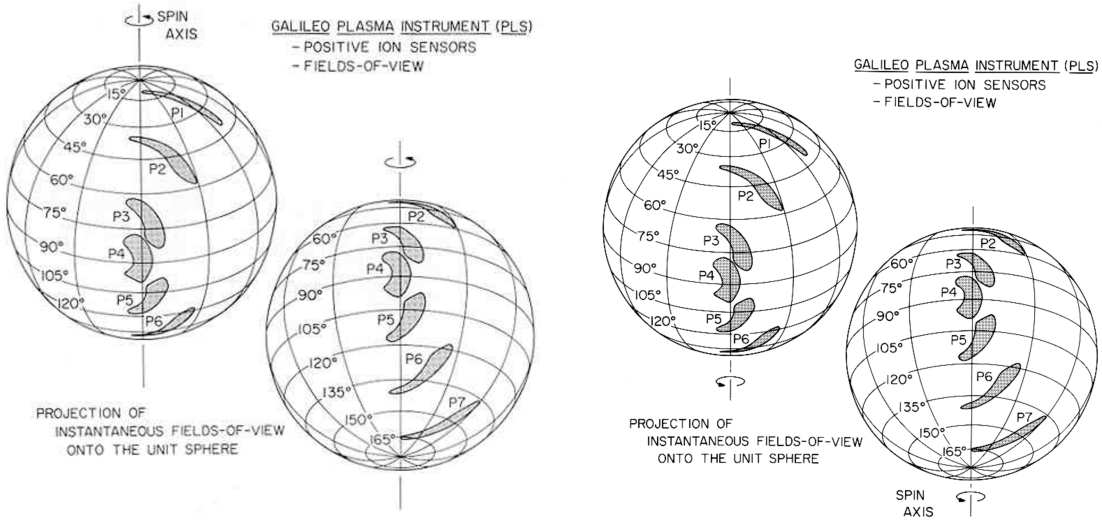


*Figure 6: Incorrect figures of spin direction and anode locations. Left is from the instrument paper, right is from a final report to NASA Grant NNG05GJ23G. Both are wrong.*

In Figure 7 we show the orientation that we believe to be correct. Galileo is spinning around its +Z vector in a right-handed sense, where the big (sadly broken) communications disk pointing ~Earthward is located at the –Z end nearest anode 7. That is, if you were standing on Earth's north pole and looking at the bottom of Galileo, the magnetometer boom would appear to be rotating clockwise.

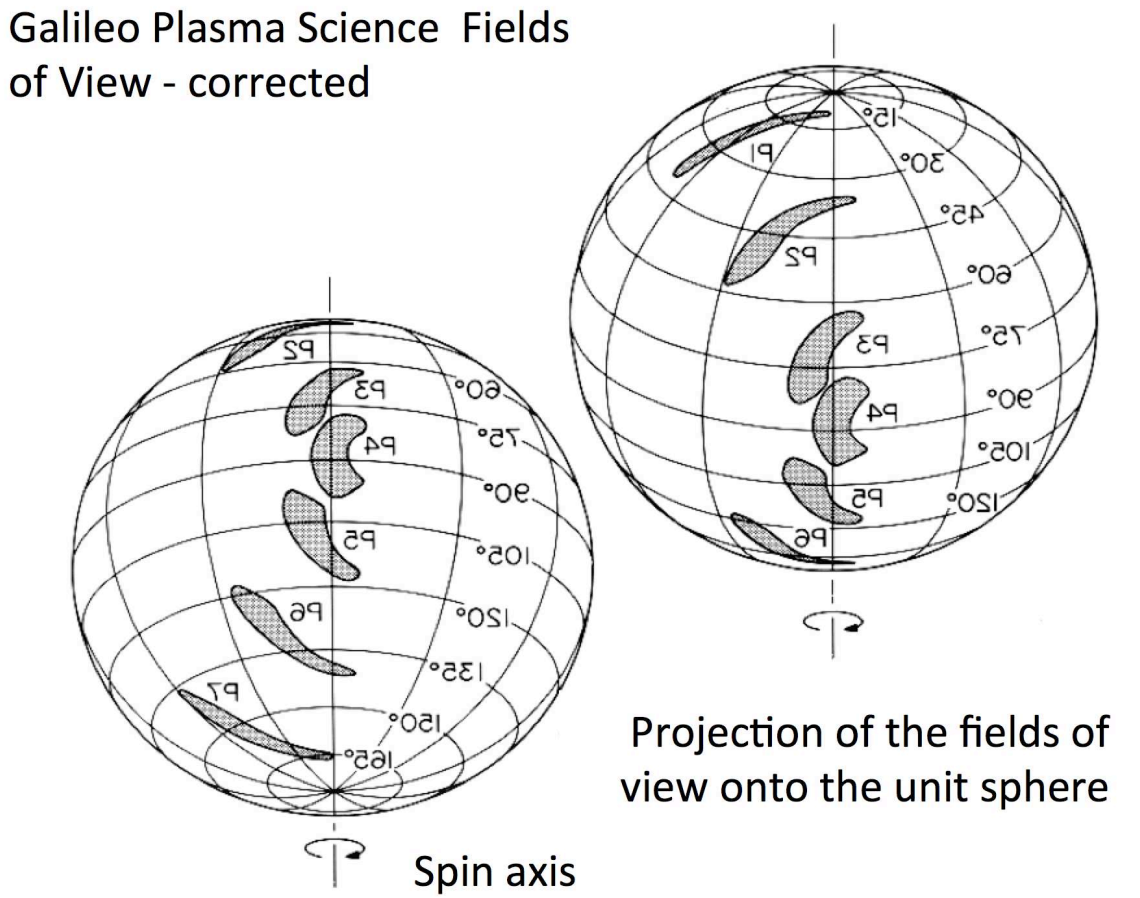


*Figure 7: Fields of view of the 7 different anodes of the Galileo PLS instrument. Note that the writing is shown backwards because of the flipping of the orientation of the coordinate system relative to the originally published figure.*

The spin-phase for the data set is given in the SECTOR_ID parameter of the level 3 PDS data. This is a 1-byte value of 0 to 255. Lower and medium resolution data begin energy sweeps (azimuths) when SECTOR_ID is 0, 64, 128 or 196. High resolution data begin energy sweeps when SECTOR_ID is 0, 32, 64, 96, 128, 160, 192 or 224. To put this into context of spacecraft orientation, SECTOR_ID = 0 is when (the center of) PLS detector 1 and detector 7 are in the plane containing ECL-50 'north', which is essentially +Z in SPICE frame ECLIPB1950. See the next section for more details.

The PDS description of the field of view of each anode is always reversed from the theta/phi values given – see section 12 for details.

## 6. Co-ordinate Systems Used for Galileo: EME-50, ECL-50 and IRC

Most published PLS data use the Inertial Rotor Co-ordinate (IRC) frame. This is a despun spacecraft centered frame aligned with Galileo's spin axes. However, its specific definition is different for different instruments and we have been unable to locate rigid definitions. All instruments agree on using the spacecraft spin axis for +z, but definitions located by these authors are no better than '+y is approximately dawnward'. The magnetometer team use a right-handed IRC frame where '+x is approximately southward'. However the PLS team have +x as 'approximately northward' and appear to use a left-handed frame, so that +y is also approximately dawnward. Without knowing a precise definition it is hard to compare plasma moments in an IRC co-ordinate in the spacecraft frame with the plasma parameters of this study that are in planet centered co-ordinates that account for spacecraft orientation and velocity, i.e. IRC +y may be radially outward or radially inward depending if Galileo is on the dusk or dawn side of Jupiter.

Recent missions tend to use the NASA NAIF (Navigation and Ancillary Information Facility) J2000 frame as their base frame for work, however Galileo pre-dates use of NAIF's software and their SPICE kernels. Instead the Galileo mission used four co-ordinates to describe spacecraft orientation and spin phase, which are Rotor Right Ascension (RA), Rotor Declination (Dec), Rotor Spin and Rotor Twist. Three of these are giving in the EME-50 co-ordinate system (Earth Mean Equatorial, equinox 1950) and one is in the ECL-50 co-ordinate system (Earth Mean Ecliptic, equinox 1950). We are thinking that the issue with some past Galileo work has been assuming all four were EME-50 co-ordinates, resulting in radial and poloidal ($V_r$ and $V_\theta$) components appearing to have a sinusoidal dependence with the spacecraft's local time.

The original RA, Dec, Spin and Twist values are freely available at the Planetary Data System's website, in the PDS volume: GO-J-POS-6-REDR-ROTOR-ATTITUDE-V1.0
Since then the NAIF team has created SPICE kernels for Galileo's position and orientation based on these, however this does not provide spin-phase directly. One can now use NAIF's SPICE kernels and code to calculate position, orientation and Galileo spin-rate, then with some geometry can calculate spin-phase by finding the ECL-50 'north pole' in your chosen reference frame. The following bulleted sections (next page) are a summary of the important information.

Galileo Co-ordinate Systems and SPICE:

- Galileo used two co-ordinate systems, EME-50 and ECL-50.
- EME-50 is frame 'FK4' ("Fundamental Catalog (4)") in SPICE.
    - Although EME-50 is often a catchall term for several 1950 reference frames, FK4 is the SPICE frame Galileo teams used for EME-50.
- ELC-50 has no SPICE frame.
    - Previous Galileo work used an ELC-50 north pole vector expressed in EME-50 co-ordinates, then used geometry to calculate spin phase angle.
- SPICE frame 'B1950' is FK4 improved, but so minor (≈½ arc second ≈ 0.00014 degrees) that for Galileo PLS pointing use we can consider B1950 ≅ FK4.
- SPICE frame ECLIPB1950 is then ≅ ECL-50.
- SPICE kernels can now be used without having to use ROTOR RA/DEC/SPIN/TWIST values.

ROTOR co-ordinates, RA, DEC and SPIN vs. TWIST:

- All are in units of radians.
- ROTOR Right Ascension and Declination gave spin vector in EME-50.
- ROTOR TWIST is then the rotation from the plane containing 'EME-50' north.
- ROTOR SPIN is the rotation from the plane containing 'ECL-50' north, used onboard to describe the difference between the spun and despun sections.
    - Seems the team uses EME-50 for navigation purposes, but ECL-50 to describe the rotation between the spun/despun section.

Spin-Phase from PLS SECTOR_ID value:

- SECTOR_ID is a 1-byte value, 0 – 255 to cover 1 spin.
    - Due to a software bug in creating PDS files, PLS values in photo-electron modes can go over 255, then use modulus 256 on the value, hence 256 = 0, 257 = 1, etc.
- SECTOR_ID is equivalent to ROTOR SPIN (not ROTOR TWIST).
- SECTOR_ID = ROTOR SPIN * 256/2π, rounded down to a whole number.
- SECTOR_ID = 0 is when PLS detector 1 and detector 7 are in the plane containing ECL-50 'north', which is +Z in SPICE frame ECLIPB1950.

## 7. Quantization of Counts

The returned counts/sec in the level 3 data file used are converted back to counts per accumulation for forward fitting of the data, as this is the unit returned by the instrument. However, that number has to be compressed from a 2-byte or bigger number to a 1-byte value for transmission via a look up table, which loses resolution. That is, a returned value of 240 really only tells you that PLS counted 240 to 247 counts per that accumulation period, but we do not know where in that range. Appendix C gives a table with the full compression table used and lower and upper values of each range. Not all available 256 values of a 1-byte number are used, but the 224 ones that are used are given.

Usually the lower value in the range is used for all science. For the reduced chi-square we use the lowest values for the signal and background on the numerator. But use the highest value for the signal and background in the denominator used for Poisson statistics of uncertainty. The reason for this is that it is better to overestimate than to underestimate uncertainty. E.g. returning to the earlier example, if there is no background and a returned value is 240, then the uncertainty on that value of 240 is the square root of 247, not the square root of 240.

## 8. Maxwellian Forward Model Fit

The Forward Model used is a straightforward Maxwellian fit of one isotropic ion species moving in three dimensions. We assume spacecraft potential is zero (and have no suitable Mode 1 data to say otherwise). Another assumption used is that we know the mass (amu) and charge (e) of the ion species, using a function dependent on radial distance for both (see below). With these assumptions we can calculate all other values required (e.g. calculate ion velocity based on the measured energy step of a given eV/q).

The coordinate system used for this analysis is Jupiter de-Spun Sun (JSS) defined as:

$Z$ = unit vector of Jupiter spin axis

$Y = Z \times R_{JupiterToSun}$

$X = Y \times Z$

Where: $R_{JupiterToSun}$ is the unit vector of the Jupiter to Sun line, but aberration corrected for one-way light time and stellar aberration (in SPICE code use `abcorr = 'LT+S'`, or use SPICE command *et2lst* with `type = 'PLANETOCENTRIC'`). Failure to include this correction results in noon Local Time not being precisely along +X, although the difference is < 2 milli-degrees (or < 0.6 seconds Local Time), far below the ability of PLS data to notice.
This work uses spherical co-ordinates in the JSS frame: $\theta$ is the co-latitude from +Z, and $\phi$ is the azimuthal angle, $\phi = 0°$ for +X, and positive in a direction towards +Y.

Five free parameters are used in the single ion species fit: density, (isotropic) temperature and three velocity components. A model of PLS was coded that, given the five free parameters, PLS calibrations and Galileo position/orientation information for that merged-spin, would simulate the counts per accumulation that each energy step at each azimuth of the spin should measure. This simulated data is compared with the actual observed data, and the free parameters iterated repeatedly until a best fit is found. To define best fit we minimize a reduced Chi-squared form. Equations used are described below.

Counts per accumulation is found from the phase space density at a given energy step and look direction:

$$\frac{Counts}{Accum.} = \text{ACCUM\_TIME} * G * v^4 * f$$

where *G* is the geometric factor including efficiency (see Table 2), *f* is phase space density and *v* is velocity calculated from:

$$E_{table} = \frac{mv^2}{2q} \quad \Rightarrow \quad v = \sqrt{\frac{2qE_{table}}{m}}$$

*where* $E_{table}$ is the eV/q value of the energy table for that particular anode and energy step (see Table 2 for the values used in this study).

Phase space density itself is the Maxwellian form, and in three dimension with isotropic temperature is given as:

$$f = n\left(\frac{m}{2\pi kT}\right)^{\frac{3}{2}} \exp\left(-\frac{m\left(u_r - v_r\right)^2}{2kT} - \frac{m\left(u_\theta - v_\theta\right)^2}{2kT} - \frac{m\left(u_\phi - v_\phi\right)^2}{2kT}\right)$$

where *n* is density, *m* is mass, *T* is temperature, *k* is the Boltzmann constant, *v* is the velocity of Galileo, *u* is the bulk flow of the plasma and both *u* and *v* have three components: r, θ and ϕ.

The reduced Chi-squared form for 5 free parameters with *n* data points is:

$$\chi_r^2 = \frac{1}{n-5}\sum_{i=1}^{n}\frac{\left(Signal_i - Background_i - Simulation_i\right)^2}{\sigma_i^2} + \left\{\text{Any constraint penalty}\right\}$$

where $\sigma_i^2 = Signal_i + Background_i$ according to Poisson statistics, unless they total zero in which case $\sigma_i^2 = 1$; that is the full formula is:

$$\sigma_i^2 = \sigma_{Signal_i}^2 + \sigma_{Background_i}^2 = \begin{cases} Signal_i + Background_i & \text{if } Signal_i + Background_i > 1 \\ 1 & \text{if } Signal_i + Background_i = 0 \end{cases}$$

We fit one ion species, with an assumed representative mass and charge based on the composition from the physical chemistry model of Delamere et al. [2005]. For coding purposes, the following numbers were used for fixed radial distance (R), and then m and q were separated linearly interpolated from these and the interpolated value rounded to two decimal places for the m:q used in the fitting code.

```
R = [0          , 5          , 5.5        , 6          , 7          ,
     8          , 9          , 10         , 15         , 20         ,
     30         , 300        ]
m = [27.79381443, 27.79381443, 27.41573034, 23.98694943, 23.85507246,
     23.97231834, 23.95563771, 23.95563771, 23.95563771, 23.95563771,
     23.95563771, 23.95563771]
q = [1.025773196, 1.025773196, 1.050561798, 1.471451876, 1.603260870
     1.685121107, 1.713493530, 1.713493530, 1.713493530, 1.713493530
     1.713493530, 1.713493530]
```

The model code took the free parameters as inputs and immediately rounds them to the 3rd decimal place before continuing with the simulation and returning a value calculated from the reduced chi-squared value for minimization. To speed up the minimization (in addition to only using 3 decimal places in units of $cm^{-3}$, eV and km/s) the model included limits and constraints. If a constraint was hit then the model adds

on a multiple of $10^6$ to the reduced chi-squared value. e.g. if a negative density (neg. den.) is tried:

*Reduced-Chi-squared returned value = Reduced-Chi-squared + $10^6$(1 + abs[neg. den.])*

This form returns a values that is always greater than $10^6$ and that can still be minimized to encourage the fitting code to try a smaller negative value on its path to returning to positive densities (as opposed to just returning "Reduced Chi square + $10^6$" which would not distinguish between negative values for density).

Given the sparseness of Galileo data, often jumping energy steps, further constrains forced the peak signal of the simulated distribution to be within 1 anode of (or the same anode as) the peak anode of the measured signal (i.e. maximum counts above background). Likewise, the energy step of peak signal of the simulated distribution must be within 4 energy steps of the observed energy step of the peak signal. This ensures the fitted simulated distribution peaks in a field of view that broadly matches the field of view of the instrument that not only contained data but also contained the peak signal (rather than a field of view that was not sampled by Galileo during this merged-spin). We employed limits to prevent the minimization from routine looking in pointless places from minus-infinity to plus-infinity. These following limits were used when Galileo was <30 $R_J$ to defined allowed search ranges:

- $V_r$ and $V_\theta$ limits were -200 to +200 km/s
- $V_\phi$ limits were -200 km/s to the smaller of +1000 km/s or 120% rigid corotation
- Temperature limits were 0.001 to 20000 eV
- Default density limits of 0.001 to 10000 $cm^{-3}$, unless:
  - If Galileo < 10 $R_J$ then lower density limit of 1 $cm^{-3}$
  - Else if 20 $R_J$ < Galileo < 30 $R_J$, upper density limit 10 $cm^{-3}$
  - Else if 12 $R_J$ < Galileo < 20 $R_J$, upper density limit 100 $cm^{-3}$

These criterions show a gap of 10-12 $R_J$ where a more appropriate lower or upper limit could have been used, but this not did affect any results. One might wonder why the 120% rigid corotation limit was implemented as it prevents the code finding faster flows. If the flow were faster, the limit would have been hit. In earlier runs this criterion was set at a 200% rigid corotation limit – however no data were ever found exceeding corotational speeds.

Once a best fit set of free parameters had been found to match the observed data, uncertainties on those free parameters were calculated. These uncertainties were calculated in the standard text book way, being the square roots of the diagonal of the covariance matrix. The covariance matrix itself is the matrix inverse of the alpha matrix, which is half the curvature matrix that defines the chi-square well at the best fit location, see section 11 for more details.

## 9. Pre-pruning the Data Before Applying the Forward Model

Carrying out a forward model requires the data to have a shape that can be fit. If there are too few counts or sporadic counts, i.e. 5 neighboring energy steps with data have 0, 10, 0, 5, 0 counts, then the fit will be poor as it is not a smooth singular shape. The code will find a mathematical fit, always, but it will not always be meaningful. For this reason, we only include merged-spins where the peak counts are above a threshold. This requirement alone removed much of the data beyond 30 $R_J$ where few counts were measured.

In order to be as close to the original observed data as possible, the PDS data in units of counts/second (provided in the PDS to a few decimal places) was reverted back to counts per accumulation period. This process was merely dividing counts/second by the ACCUM_TIME, and then rounding to the nearest whole number.

Background is then calculated from these values, and a signal of counts above background is used to see if the merged-spin is worth processing. The anode and energy step with the highest signal above background is then found, as that indicates the look direction that measures the largest signal (looking into the flow).

The (sub-)corotational ion beam is very narrow and only seen in a few anodes. For instance, when PLS looks parallel to the corotation direction it does not observe any counts. It is pointless to include these energy sweeps that contain no useful information. With this in mind, we identify the direction with the peak counts above background and keep the data from that anode and its immediate neighboring anodes. For instance, if anode 5 had the observed peak flow we keep anodes 4, 5, and 6, and ignore anodes 1, 2, 3, and 7, which do not contain any signal. If the peak signal is on an end anode, then obviously there is only one neighboring anode to be used. However, if the neighboring anode has no data (i.e. all fill-values due to not having a data record returned for it), then the next nearest neighbor anode is included.

In addition, we remove particular energy steps of those anodes that are not within a specific angular distance from the energy step/anode of peak count above background. For Modes 2 and 3 (ACCUM_TIME of 0.5000 or 0.2667 seconds) that angle is 135 degrees (90*1.5), while for Mode 4 (ACCUM_TIME of 0.1500 seconds) that angle is 67.5 degrees (45*1.5). In both cases this is 1.5 times the phi angular distance of one sweep of energies. In essences this gives us nearest neighbor anodes and nearest neighbor energy sweeps to the peak flow direction as seen by PLS.

Then, as a final check, we confirm the signal is strong enough that a meaningful fit may be viable. For this two things are insisted upon:

1. The peak signal (counts above background) must be at least 10 counts/accumulation.
2. There must be at least 5 values that are not fill values, i.e., there must be at least 5 point to fit.

The former sounds very low, but does remove a lot of data. With a peak from 10-100 counts/accumulation the shape may still be too poor to get a physically representative fit. However, the post-pruning catches the outliers. The second criterion is simply a requirement for the fitting process: we fit 5 parameters, therefore, must have at least 5 data points. However, there are merged-spins that fail this criterion, mostly when many of the azimuth records were not returned.

## 10. Post-pruning the Forward Modeled Data

A forward model fit will always return a 'best' fit, but is it good enough? Some minimization fitting routines will exit once a number of iterations are met, or if it thinks a tolerance has been met.

Luckily, these are easy to spot by examining the covariance matrix and uncertainties of the fit. The 1-sigma uncertainties on each free parameter are provided by the square root of the covariance matrix of the fit. If the fit exited early, due to a tolerance or iteration limit, the parameter search will not be at the true minimum of parameter space and it is likely that one of the elements of the diagonal of the covariance matrix is a negative number. When this is square-rooted to give a 1-sigma value you either get a complex number, a not-a-number, a zero, or the code crashes, depending on software platform.

If any of the 1-sigma uncertainties of the 5 parameters is returned as 0 or complex then the whole fit is considered bad. On some occasions simply re-running the fit will allow it to converge to the minimum on its second or third try. For this reason, we tried every initial failed fit up to 10 times. If it was still failing then the merged-spin was considered bad and ignored. This is usually due to any of the following: Data too sparse so insufficient shape to be fit, too few counts, a huge count in one energy step but none in the others (basically a delta function) or a merged spin that was missing data from the peak flow and only provided up ramps towards where the peak would have been.

In a similar vein, any uncertainty that is less than 0.003 means the whole fit is bad. Recall we fit to 3 decimal places. If the uncertainty is too small then it is considered unrealistic. In addition, the uncertainties for $V_\phi$, n and T all had to be in a percentage range of 0.75% to 100 % of the fitted parameter. Parameters $V_r$ and $V_\theta$ were exempted

from this percentage check as their value often hover near zero, and can be negative or positive and their uncertainties are often much larger than their fitted value.

During the fitting process, we set limits on the ranges of each free parameter (see section 8). Having range limits such as these speeds up convergence by ignoring unphysical or unlikely values (e.g. density and temperature can never be negative).

As such, checks were put in to ensure the fitted parameters were less than 95% of all upper limits, greater than 95% of lower limits for the velocities (lower limits being negative or 0, e.g. if lower limit was -200 km/s then must be > -190 km/s), or greater than 3x the lower limit for density and temperature. If these checks were violated then re-running the fit often resolved it, similar to if the fit stopped early due to a tolerance being met. If it continued to hit a limit then the limits were adjusted to be larger and the code was re-run until a safe fit was found.

Fits with a Reduced Chi-squared value less than 0.8 were excluded, as that is a sign that there was no signal to fit. Conversely, we have no limit on how large a reduced chi-square value can be as long as it is less than $10^6$ (an indication that a constraint was hit in the fitting). In regions of high background the reduced chi-squared value can be high, but still give a good fit. If the fit is terrible then the percentage error checks are sufficient to exclude them.

Any interval when Galileo was within 10 $R_{moon}$ of a Galilean moon was excluded. During a moon encounter the plasma environment can change greatly between each spin. The plasma conditions are not constant during a merged spin. A fit must assume the plasma conditions are stable throughout. The cadence of the instrument is too slow for moon encounters.

To summarize, the post-pruning checked that:

- Uncertainties were not complex numbers but real
- All fitted parameter uncertainties > 0.002 of their respective units
- Galileo was not near a moon
- Reduced Chi-Square > 0.8
- Reduced Chi-square < $10^6$ ($\geq 10^6$ meaning a constraint was hit in the fit)
- Fitted velocities were >95% of the respective velocity lower limits
- Fitted density and temperature were > 3x their respective lower limits
- Fitted velocities, density and temperature were <95% of their respective upper limits
- $V_\phi$ uncertainty must be in the range of 0.75% to 100% of the fitted $V_\phi$ value.
- Density uncertainty must be in the range of 0.75% to 100% of the fitted density value.
- Temperature uncertainty must be in the range of 0.75% to 100% of the fitted temperature value.

## 11. Relationship Between Parameter Uncertainties and Chi-Squared.

The basic reduced Chi-squared function is as follows, which we'll rename *Z* for clarity of later equations. The observed data (having already removed the observed background) is $O_i$ with uncertainty $\sigma_i$, while the simulation is $S_i$. The free parameter vector fed to the simulation is $\bar{p}$, which has $\upsilon$ elements (5 in this case).

$$Z = \chi_r^2 = \frac{1}{n-\upsilon}\sum_{i=1}^{n}\frac{\left(O_i - S_i\left[\bar{p}\right]\right)^2}{\sigma_i^2}$$

$Z$ is minimized and near the best fit location the hyper surface in parameter space is quadratic to an excellent approximation. This can be seen by using a Second Order Taylor Series Expansion of Z around the best fit parameters (indicated by the subscript 0):

$$Z \cong Z_0 + \sum_{i=1}^{\upsilon}\frac{\partial Z_0}{\partial p_i}\left(p_i - p_{i0}\right) + \frac{1}{2}\sum_{i=1}^{\upsilon}\sum_{j=1}^{\upsilon}\frac{\partial^2 Z_0}{\partial p_i \partial p_j}\left(p_i - p_{i0}\right)\left(p_j - p_{j0}\right)$$

At the best fit location in parameter space the value of Z has a minimum value of $Z_0$, hence the first derivative is zero, and thus resultant description of the hypersurface near the best fit is quadratic.

$$Z \cong Z_0 + \frac{1}{2}\sum_{i=1}^{\upsilon}\sum_{j=1}^{\upsilon}\frac{\partial^2 Z_0}{\partial p_i \partial p_j}\left(p_i - p_{i0}\right)\left(p_j - p_{j0}\right)$$

Standard text books, such as *Bevington & Robinson* (2003), provide uncertainties of fitted parameters by providing the covariance matrix; the square roots of the diagonal of the covariance matrix are the uncertainties for each of the free parameters.

Uncertainties to the fitted parameters of this study were found this standard way, where the code calculates the Hessian matrix of the fit on free parameter vector $\bar{p}$, which is of size $\upsilon$ by $\upsilon$:

$$\text{Hessian Matrix} = \overline{H} = \begin{bmatrix} \frac{\partial^2 Z}{\partial p_1^2} & \frac{\partial^2 Z}{\partial p_2 \partial p_1} & \cdots & \frac{\partial^2 Z}{\partial p_\upsilon \partial p_1} \\ \frac{\partial^2 Z}{\partial p_1 \partial p_2} & \frac{\partial^2 Z}{\partial p_2^2} & \cdots & \frac{\partial^2 Z}{\partial p_\upsilon \partial p_2} \\ \vdots & \vdots & \ddots & \vdots \\ \frac{\partial^2 Z}{\partial p_1 \partial p_\upsilon} & \frac{\partial^2 Z}{\partial p_2 \partial p_\upsilon} & \cdots & \frac{\partial^2 Z}{\partial p_\upsilon^2} \end{bmatrix}$$

The alpha matrix ($\overline{\alpha}$, also known as the curvature matrix – see the Taylor Series expansion for the similarity) is merely half the Hessian matrix, and finally the covariance matrix, $S^2$, is the matrix inverse of the alpha matrix.

$$\overline{\alpha} = \frac{\overline{H}}{2}$$

$$\overline{S^2} = \overline{\alpha}^{-1}$$

Finally, the uncertainty of the $i^{th}$ free parameter (the $i^{th}$ element of vector $\overline{p}$) is $\sqrt{S_{i,i}^2}$. See *Wilson* (2015) for more details of this standard process and example code.

## 12. Instrument Calibration

The detector look directions found in the main PDS PLS volume were used for this study, under the CALIB directory, file DET_LOOK.TAB, copied here, despite their description being incorrect:

| Detector | Theta | Phi |
|---|---|---|
| 1 | 20.0 | 0.0 |
| 2 | 50.0 | 30.0 |
| 3 | 70.0 | 40.0 |
| 4 | 90.0 | 45.0 |
| 5 | 110.0 | 40.0 |
| 6 | 130.0 | 30.0 |
| 7 | 160.0 | 0.0 |

The corresponding LBL file states these are look directions in degrees of the center of the anode's (=detector) field of view. The description for Phi is provided as: "*Azimuthal angle measured in the spin plane from the +X axis towards the +Y axis of the nominal detector field-of-view.*" Here the X and Y (and Z to follow) axes stated are in spacecraft co-ordinates. The description for Theta however is "*Polar angle measured from the spacecraft spin axis (-Z) of the nominal detector field-of-view.*" This is **incorrect**. The Theta angles are actually from the spin axis +Z. We suspect this confusion comes from the confusion in spin direction mentioned earlier, however these angles are confirmed

as spin axis is 0 degrees theta and anti-spin is at 180 degrees. The big communication dish is at 180 degrees theta, nearest detector 7.

For our code we converted Theta and Phi to be analogous to spacecraft latitude and longitude. Longitude is exactly equivalent to Phi above, whereas latitude is "90 - Theta" degrees. As such, the latitudes used for anodes 1 to 7 were +70, +40, +20, 0, -20, -40 and -70 degrees respectively.

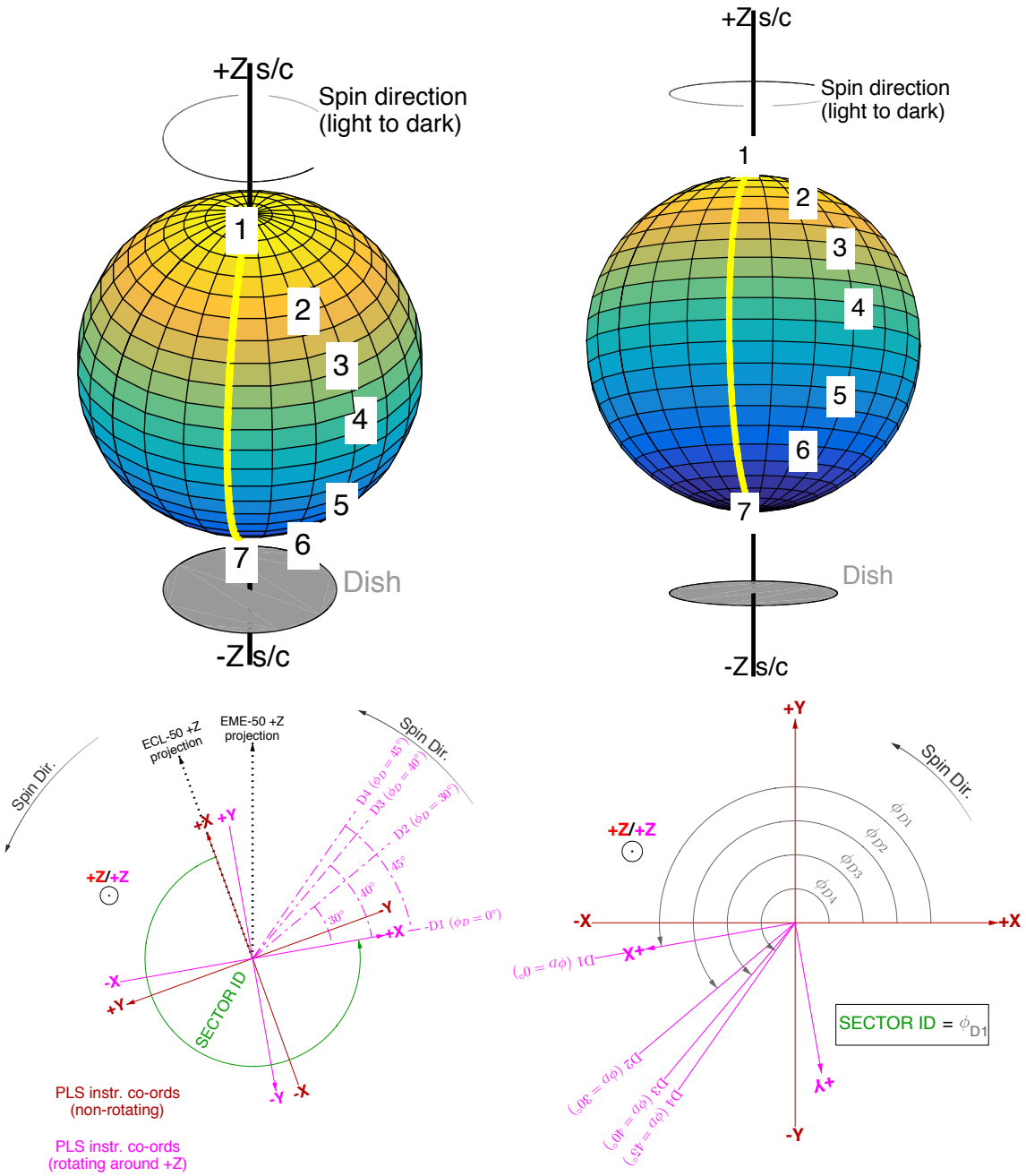


*Figure 8: Cartoon of anode placement on sphere spacecraft (tops, anode 4 leads each spin) and map of spinning and despun (non-rotating) PLS co-ordinate systems (bottoms).*

For completeness (although not used in this study) there are upper and lower values for the width in Theta of each anode in the PLS instrument paper's table 1 (copied in *Table 1* here too).

```
SC_Latitude_upper = 90-[  9  35  62  78  97 118 136]; %anode 1 to 7
SC_Latitude_lower = 90-[ 41  59  84  99 119 141 166]; %anode 1 to 7
```

For plasma parameter calculations we need to convert to a despun spacecraft frame. Here +Z is along the spacecraft spin axis (same as for the spinning spacecraft frame above), while +X is perpendicular to +Z such that the X-Z plane is parallel to ECL-50 +Z; that is +X despun spacecraft is roughly pointing 'north' in ECL-50. +Y completes the right-handed set, pointing approximately duskward. Spin phase is 0 when along despun +X and increases towards despun +Y (i.e. increases in the opposite direction of spin). Anode 4 leads the anodes in a spin, while the SECTOR_ID value increases as Galileo spins, so we need to use the negatives of the values (that is change the sign) to get a despun longitude start, middle and end angle per energy step as follows:

```
SC_Anode_phi = [ 0, 30, 40, 45, 40, 30,  0]; %anode 1 to 7

phase = Sector_ID*360/256; % Sector_ID from the PDS file into Degrees

angle_start = -SC_Anode_phi(anode) - phase;
% minus everything as phase angle is in opposite direction to spin

% Add on 1 accumulation period, using real s/c spin period
angle_end = angle_start - ACCUM_TIME*360/spin_time;

% center value is half an ACCUM_TIME later
angle_mid = angle_start - ACCUM_TIME*360/spin_time/2;
% minus everything as phase angle is in opposite direction to spin
```

where `anode` is 1 to 7, `ACCUM_TIME` is accumulation period in seconds of each step (e.g. 0.500, 0.2667, 0.1500s) and `spin_time` is the spacecraft spin period (in seconds) at the given time (approximately 19 seconds, the exact value can be pulled from NAIF's SPICE for a specific time of interest).

## 13. Notes on the PLS Sectors

In the PDS volume used for this study, PLS_CALIBRATION.TXT in the CALIB directory has lots of useful information. However it states:

*The AACS rotor spin angle is an integer number in the range 0-255. It is zero when the spacecraft X-axis is pointed at (or near) the south ecliptic pole and increases as the spacecraft rotates. The rotor spin angle may be converted to an angle in the range 0-360 degrees with the equation:*

*angle = (AACS rotor spin angle) * (360/256)*

*The fields-of-view of the PLS detectors are offset by 45 degrees from the spacecraft X-axis in the X-Y plane. So when the rotor spin angle is zero (0) the fields-of-view are making a +45 degree angle with respect to the X-axis in the X-Y plane. This 45 degree offset is not included in the AACS rotor spin angle provided in the RDR data files.*

*To compute the rotational angle from the north ecliptic pole to the velocity vector of the plasma particles entering the PLS field-of-view:*

*velocity angle = 45 + [ (AACS rotor spin angle) * (360/256) ]*

This snippet from that document has several inconsistencies. Firstly, do not confuse rotor spin angle with Sector_ID, which is zero when near the north ecliptic pole.
It also suggests adding on a 45 degree offset to get proper angles – yet this is the only document that mentions this.

This study does not add any offset to phi. However these authors tried adding on (and also removing) multiples of 45 degree offsets to see what would happen – and the results were unphysical. The data tells us there is no offset. What we suspect happened is that if you use anode 4 as your zero point for Sector_ID crossing ECL-50 north (rather than anodes 1 & 7 used in this study) then there is a 45 degree offset as anode 4 leads anodes 1 & 7 by 45 degrees. However, we recommend using the theta, phi and Sector_ID equations presented in this document.

## 14. Tables of Geometric Factors & Spice Kernels

Look directions, energy resolutions and geometry factors (that include efficiencies) to be used can be found in Table 1 of the PLS instrument paper, and copy/pasted below in Table 1. The geometric values presented in this table were not used in this study.

Galileo PLS performance parameters

| Sensor | Polar angle coverage, theta | Energy resolution, DELTA E/E at FWHM | Geometric factor**, cm2 sr eV eV-1 |
|---|---|---|---|
| **Electrons** | | | |
| | Energy range: 0.9 V <= E/Q <= 52 kV | | |
| 1E | 14°-41° | 0.14 | 1.9 x 10-5 |
| 2E | 38°-62° | 0.12 | 3.7 x 10-5 |
| 3E | 58°-80° | 0.10 | 4.1 x 10-5 |
| 4E | 81°-102° | 0.08 | 5.0 x 10-5 |
| SE | 100°-122° | 0.10 | 4.1 x 10 5 |
| 6E | 121°-146° | 0.12 | 3.6 x 10-5 |
| | 142°-171° | 0.14 | 1.3 x 10-5 |
| **Positive ions** | | | |
| | Energy range: 0.9 V <= E/Q <= 52 kV | | |
| IP* | 9°-41° | 0.15 | 9.8 x 10-5 |
| 2P | 35°-59° | 0.12 | 3.5 x 10-5 |
| 3P | 62°-84° | 0.09 | 4.1 x 10-5 |
| 4P | 78°-99° | 0.07 | 5.0 x 10-5 |
| 5P | 97°-119° | 0.09 | 4.0 x 10-5 |
| 6P | 118°-141° | 0.11 | 3.6 x 10-5 |
| 7P* | 136°-166° | 0.15 | 1.5 x 10-5 |
| **Ion composition** | | | |
| | Energy range: species dependent | | |
| | Differential (D) sensor: 0.9 V to 20 kV (H+) 0.9 V to 800 V (S+) Resolves: H+, H2, He+, O+, Na+, S+, K+ with M/DELTA M = 4.1 | | |
| | Integral (I) sensor: 10 V to 52 kV (H+) 0.9 V to 14 kV (S+) Resolves: H+, H2+, He+, O+, S+, SO2+ with M/DELTA M ~ 2.0 | | |
| 1MD*, 1MI | 11°-38° | 0.03 | 2.4 x 10-6 |
| 2MD*, 2MI | 87°-93° | 0.03 | 4.7 x 10-6 |
| 3MD*, 3MI | 142°-169° | 0.03 | 2.4 x 10-6 |

* 3-mm entrance diameter, others are 1 mm.
** Preliminary values based upon ray tracing (see text).

***Table 1: A copy of Table 1 from the PLS Instrument paper containing calibration information. Note that different geometric values were used in this study.***

A file was provided by PLS Co-I William Paterson called ANALYZER_CONSTANTS_E2.txt (dated 11/27/1990 but with comments dated 1991) that contained Fortran code to return energy tables and geometric factors. This included geometric factors (which wrap in efficiencies) that had been calibrated against PWS wide-band data during Earth Fly-bys and Venus fly-bys. Most of those iterations of improved geometric factors were commented out with the final best values left in. This study used the final values (Table 2), where p+ refers to the ion detectors (Analyzer A is the odd anodes, B the even) and e- the electron detectors (not used in this study but here for completeness).

```
    Detector      p+       e-
       1        3.0E-5   7.3E-6   % Units are cm^2 sr eV/eV
       2        12.E-6   2.7E-5   % These Geometric factors include
       3        11.E-6   16.E-6   %  efficiency.
       4        16.E-6   3.0E-5
       5        14.E-6   2.7E-5
       6        13.E-6   3.7E-5
       7        3.3E-5   4.5E-6
% Analyzer A is anodes 1,3,5,7, while Analyzer B is anodes 2,4,6
% Energy units are eV/q
```

| E-Step | ANALYZER A | | ANALYZER B | | E-Step | ANALYZER A | | ANALYZER B | |
|---|---|---|---|---|---|---|---|---|---|
| | p+ | e- | p+ | e- | | p+ | e- | p+ | e- |
| 00 | 0.9 | 0.9 | 0.9 | 0.8 | 32 | 251.3 | 244.4 | 244.3 | 227 |
| 01 | 1.1 | 1.2 | 1.1 | 1 | 33 | 309.8 | 301.4 | 302.9 | 281.3 |
| 02 | 1.4 | 1.4 | 1.4 | 1.3 | 34 | 379.4 | 369 | 372.2 | 345.8 |
| 03 | 1.7 | 1.7 | 1.7 | 1.6 | 35 | 461.3 | 448.7 | 454.4 | 422.1 |
| 04 | 2.1 | 2 | 2 | 1.9 | 36 | 549 | 534 | 549 | 510 |
| 05 | 2.5 | 2.4 | 2.5 | 2.3 | 37 | 695.4 | 676.4 | 686.3 | 637.5 |
| 06 | 3 | 2.9 | 3 | 2.8 | 38 | 841.8 | 818.8 | 823.5 | 765 |
| 07 | 3.6 | 3.5 | 3.6 | 3.3 | 39 | 969.9 | 943.4 | 960.7 | 892.5 |
| 08 | 4.3 | 4.2 | 4.2 | 3.9 | 40 | 1153 | 1121 | 1153 | 1071 |
| 09 | 5.1 | 5 | 5.1 | 4.7 | 41 | 1363 | 1326 | 1363 | 1266 |
| 10 | 6.1 | 5.9 | 6.1 | 5.6 | 42 | 1647 | 1602 | 1638 | 1521 |
| 11 | 7.3 | 7.1 | 7.2 | 6.7 | 43 | 1962 | 1908 | 1958 | 1819 |
| 12 | 8.6 | 8.4 | 8.6 | 8 | 44 | 2333 | 2269 | 2324 | 2159 |
| 13 | 10.3 | 10 | 10.3 | 9.5 | 45 | 2743 | 2668 | 2732 | 2538 |
| 14 | 12.2 | 11.9 | 12.2 | 11.3 | 46 | 3221 | 3133 | 3202 | 2975 |
| 15 | 14.5 | 14.1 | 14.5 | 13.5 | 47 | 3843 | 3738 | 3788 | 3519 |
| 16 | 17.4 | 16.9 | 17.3 | 16.1 | 48 | 4575 | 4450 | 4575 | 4250 |
| 17 | 20.6 | 20.1 | 20.6 | 19.1 | 49 | 5472 | 5322 | 5490 | 5100 |
| 18 | 24.5 | 23.8 | 24.4 | 22.7 | 50 | 6533 | 6355 | 6533 | 6069 |
| 19 | 29 | 28.2 | 29 | 26.9 | 51 | 7777 | 7565 | 7777 | 7225 |
| 20 | 34.3 | 33.4 | 34.3 | 31.9 | 52 | 8821 | 8580 | 8821 | 8194 |
| 21 | 40.7 | 39.6 | 40.7 | 37.8 | 53 | 10614 | 10324 | 10614 | 9860 |
| 22 | 48.3 | 46.9 | 48.2 | 44.8 | 54 | 12810 | 12460 | 12810 | 11900 |
| 23 | 57.2 | 55.6 | 57.1 | 53.1 | 55 | 15189 | 14774 | 15189 | 14110 |
| 24 | 67.3 | 65.5 | 67.4 | 62.6 | 56 | 17934 | 17444 | 17971 | 16694 |
| 25 | 79.8 | 77.6 | 79.8 | 74.2 | 57 | 21374 | 20790 | 21356 | 19839 |
| 26 | 94.6 | 92 | 94.5 | 87.8 | 58 | 25254 | 24564 | 25254 | 23460 |
| 27 | 112 | 108.9 | 112 | 104 | 59 | 29829 | 29014 | 29829 | 27710 |
| 28 | 132.4 | 128.8 | 132.5 | 123.1 | 60 | 34770 | 33820 | 34770 | 32300 |
| 29 | 156.8 | 152.5 | 156.9 | 145.8 | 61 | 40626 | 39516 | 40443 | 37570 |
| 30 | 185.8 | 180.7 | 185.8 | 172.6 | 62 | 46665 | 45390 | 46482 | 43180 |
| 31 | 220 | 214 | 219.9 | 204.3 | 63 | 52704 | 51264 | 52521 | 48790 |

***Table 2: Actual geometric factors and energy tables used in this study.***

Note that the geometric factors used for each anode are scalar; both energy independent and unvarying over the mission.

NAIF SPICE kernels were used as the basis to get Galileo position and orientation (plus some geometry), and Table 3 lists the kernels used for this study. Two notes: there is no ck kernel for orbits 5 nor 13 as these orbits returned no data (Jupiter-Sun-Earth line) and the Iowa website for position may use s980326b.bsp instead of the version a used here.

| | | | |
|---|---|---|---|
| ck95332j_rtr.bc | cke12f_rtr.bc | cki24f_rtr.bc | ckj35f_rtr.bc |
| ckg01b_rtr.bc | cke14f_rtr.bc | cki25f_rtr.bc | |
| ckg02b_rtr.bc | cke15f_rtr.bc | cke26f_rtr.bc | mk00062a.tsc |
| ckc03b_rtr.bc | cke16f_rtr.bc | cki27f_rtr.bc | naif0010.tls |
| cke04b_rtr.bc | cke17f_rtr.bc | ckg28f_rtr.bc | pck00010.tpc |
| cke06b_rtr.bc | cke18f_rtr.bc | ckg29f_rtr.bc | |
| ckg07b_rtr.bc | cke19f_rtr.bc | ckc30f_rtr.bc | s970311a.bsp |
| ckg08b_rtr.bc | ckc20f_rtr.bc | cki31f_rtr.bc | s980326a.bsp |
| ckc09b_rtr.bc | ckc21f_rtr.bc | cki32f_rtr.bc | s000131a.bsp |
| ckc10b_rtr.bc | ckc22f_rtr.bc | cki33f_rtr.bc | s030916a.bsp |
| cke11b_rtr.bc | ckc23f_rtr.bc | cka34f_rtr.bc | |

***Table 3: List of SPICE kernels used in this study.***

## 15. Other Useful Information on Errata in PDS PLS Documents

- The instrument paper's figure showing the Galileo spin direction is wrong, as described earlier in this document. The figure given in the report about the numerical moments is different but also wrong.

- The Galileo PDS volumes CALIB files do not list Geometric Factors anywhere. The PLS Instrument paper has some early numbers, which were later improved in-flight and are quoted within this document.

- Energy tables (in the CALIB directory) differ slightly from values used here (sourced from PLS Co-I). This is probably just a typo, and occurs at energies not populated with plasma (or where zero counts are measured) in this study.

- PDS volume GO-J-PLS-5-RTS-MOMENTS-V1.0 has no CALIB directory explaining which calibrations were used for that study – however it was written up as a final report for NASA Grant NNG05GJ23G, which is publically available:
  *Refinement of Plasma Measurements from the Galileo Mission to Jupiter*
  *May 15, 2005 – September 30, 2009*
  *Principal Investigator: Dr. William R. Paterson*

- The CALIB/DET_LOOK.TAB file has the wrong sign for theta (are the polar angles relative to spin axis –Z or +Z?) as described earlier in this document.
  (PDS volume: GO-J-PLS-3-RDR-FULLRES-V1.0/CALIB/DET_LOOK.LBL)

- PDS file PLS_CALIBRATION.TXT is the only file to mention a 45 degree offset in phi to apply to all data. We believe that to be incorrect and not needed. Our testing shows that adding or removing 45 degrees gives unrealistic results.

**APPENDIX A: Information in PDS about PLS and Galileo**

## *Useful PDS volumes for Galileo PLS*

**GO-J-PLS-2-EDR-RAW-TELEM-PACKETS-V1.0**

This data set contains instrument packet files (IPFs) from the Plasma Science experiment (PLS) onboard the Galileo spacecraft during the Jupiter orbital operations phase. This data set is in a very raw, complex binary form.

SFDU format.

Has DOCUMENTS directory with Galileo files.

**GO-J-PLS-3-RDR-FULLRES-V1.0**

"This data set contains raw data from the Plasma Science instrument (PLS) on the Galileo spacecraft for all Jupiter orbits. These data have been reformatted into ASCII tables to facilitate data processing and analysis."

Text file format, used as basis for this study.

Contains counts and SECTOR_ID defined as: "AACS sector (clock angle) at start of spin-sector (0-255). In some instances, this value is greater than 255. These instance might be errors but can't be corrected at this time."

Has DOCUMENTS directory with Galileo files.

Has CALIB directory with Galileo PLS files.

**GO-J-PLS-4-SUMM-AVG-COUNTS-V1.0**

This data set contains averaged raw data from the Plasma Science instrument(PLS) on the Galileo spacecraft for all Jupiter orbits. These data have been averaged and reformatted into ASCII tables to facilitate data display and analysis.

Has DOCUMENTS directory with Galileo files.

**GO-J-PLS-4-SUMM-BROWSE-V1.0**

This data set contains spin averaged count rates from selected ion and electron channels from the Plasma Science experiment (PLS) onboard the Galileo spacecraft during the Jupiter orbital operations phase.

Has DOCUMENTS directory with Galileo files.

Seems to be data from just one anode.

**GO-J-PLS-5-RTS-MOMENTS-V1.0**

Galileo plasma moments (ion density, temperature, velocity) derived from the real-time science (RTS) data acquired by the instrument between 1996-11-04 and 1996-11-08 (inside of $30R_J$).

Velocity is in PLS IRC co-ordinates.

## *Useful PDS volumes for Galileo spacecraft*

**GO-J-POS-6-REDR-ROTOR-ATTITUDE-V1.0**

This data set contains the attitude data for the rotor of the Galileo spacecraft. The data provided cover portions of the Jupiter Approach (JA) and all orbit operation mission phases (J0-J35).

From LBL files: "Galileo AACS rotor attitude angles and a rotation matrix for converting data in Earth Mean Equatorial, epoch 1950 (EME-50) coordinates to System III [1965] coordinates. These data are from the IO 0 ORBIT and cover 1996-05-23T15:00 to 1996-06-22T23:00"

Note J0 PLS data is from December 1995, so this file does not cover it.

Has:

ROTOR RIGHT ASCENSION (EME-50 coordinates),
ROTOR DECLINATION (EME-50 coordinates),
ROTOR TWIST (Rotor twist (spin phase) angle, EME-50 coordinates),
ROTOR SPIN (Rotor spin phase angle, ECL-50 coordinates),
And EME-50 to SYSIII rotation matrix.

**GO-J-POS-6-SC-TRAJ-JUP-COORDS-V1.0**

This data set tabulates the Galileo spacecraft ephemeris in System III, Jupiter Solar Equatorial, and Jupiter Solar Magnetospheric coordinates. Data are sampled every minute near Jupiter (less frequently at large distances) for all Jupiter orbits.

Has DOCUMENTS directory with Galileo files.

Just position info, no orientation.

**GO-J-POS-6-SC-TRAJ-MOON-COORDS-V1.0**

This data set contains Galileo trajectory data in moon (Amalthea, Io, Europa, Ganymede, Callisto) centered coordinates for all of the near satellite encounters. Ephemeris data are provided every two seconds for ~ one hour about closest approach.

Has DOCUMENTS directory with Galileo files.

Just position info, no orientation.

## *Galileo Documents in PDS:*

**PLS:**
GO-J-PLS-2-EDR-RAW-TELEM-PACKETS-V1.0/DOCUMENT/PLS/PLS.PDF – PLS instrument paper
GO-J-PLS-2-EDR-RAW-TELEM-PACKETS-V1.0/DOCUMENT/PROJECT/SFDU_DOC/SFDU_DOC.HTM
GO-J-PLS-2-EDR-RAW-TELEM-PACKETS-V1.0/DOCUMENT/PROJECT/GLL3_180/IMAGES.HTM
GO-J-PLS-2-EDR-RAW-TELEM-PACKETS-V1.0/DOCUMENT/PROJECT/GLL3_280/3_280_P1.ASC
GO-J-PLS-2-EDR-RAW-TELEM-PACKETS-V1.0/DOCUMENT/PROJECT/GLL3_280/3_280_P2.PDF
GO-J-PLS-2-EDR-RAW-TELEM-PACKETS-V1.0/DOCUMENT/PROJECT/GLL3_280/3280_P2A.PDF
GO-J-PLS-2-EDR-RAW-TELEM-PACKETS-V1.0/DOCUMENT/PROJECT/GLL3_280/280P2AT2.PDF
GO-J-PLS-2-EDR-RAW-TELEM-PACKETS-V1.0/DOCUMENT/PROJECT/GLL3_310/3_310_P2.PDF
GO-J-PLS-2-EDR-RAW-TELEM-PACKETS-V1.0/DOCUMENT/PROJECT/GLL3_640/GLL3_640.HTM
GO-J-PLS-2-EDR-RAW-TELEM-PACKETS-V1.0/DOCUMENT/PROJECT/SEF_SIS/SEF_SIS.PDF

GO-J-PLS-3-RDR-FULLRES-V1.0/DOCUMENT/PLS.PDF – PLS instrument paper
GO-J-PLS-3-RDR-FULLRES-V1.0/DOCUMENT/SEF_SIS.PDF – Spacecraft Event File
GO-J-PLS-3-RDR-FULLRES-V1.0/DOCUMENT/PROJECT/SEF_SIS.PDF – same again
GO-J-PLS-3-RDR-FULLRES-V1.0/DOCUMENT/PROJECT/AR_SEF/SEF_SIS.PDF – and again
GO-J-PLS-3-RDR-FULLRES-V1.0/DOCUMENT/PROJECT/AR_SEF – timing of events per orbit
GO-J-PLS-3-RDR-FULLRES-V1.0/DOCUMENT/PROJECT/SFDU_DOC/SFDU_DOC.HTM
GO-J-PLS-3-RDR-FULLRES-V1.0/DOCUMENT/PROJECT/GLL3_180/IMAGES.HTM
GO-J-PLS-3-RDR-FULLRES-V1.0/DOCUMENT/PROJECT/GLL3_280/3_280_P1.ASC
GO-J-PLS-3-RDR-FULLRES-V1.0/DOCUMENT/PROJECT/GLL3_280/3_280_P2.PDF
GO-J-PLS-3-RDR-FULLRES-V1.0/DOCUMENT/PROJECT/GLL3_280/3280_P2A.PDF
GO-J-PLS-3-RDR-FULLRES-V1.0/DOCUMENT/PROJECT/GLL3_280/280P2AT2.PDF
GO-J-PLS-3-RDR-FULLRES-V1.0/DOCUMENT/PROJECT/GLL3_310/3_310_P2.PDF
GO-J-PLS-3-RDR-FULLRES-V1.0/DOCUMENT/PROJECT/GLL3_640/GLL3_640.HTM

**AACS:** (No Document directory – but a description in the LBL file of rotor co-ordinates/etc.)
GO-J-POS-6-REDR-ROTOR-ATTITUDE-V1.0/DATA/ROTOR_ATTITUDE/ROTATT00.LBL

**MAG:**
GOMAG_5001/DOCUMENT/MAG/MAG.PDF – MAG instrument paper
GOMAG_5001/DOCUMENT/PROJECT/SFDU_DOC/SFDU_DOC.HTM
GOMAG_5001/DOCUMENT/PROJECT/GLL3_180/IMAGES.HTM
GOMAG_5001/DOCUMENT/PROJECT/GLL3_280/3_280_P1.ASC
GOMAG_5001/DOCUMENT/PROJECT/GLL3_280/3_280_P2.PDF
GOMAG_5001/DOCUMENT/PROJECT/GLL3_280/3280_P2A.PDF
GOMAG_5001/DOCUMENT/PROJECT/GLL3_280/280P2AT2.PDF
GOMAG_5001/DOCUMENT/PROJECT/GLL3_310/3_310_P2.PDF
GOMAG_5001/DOCUMENT/PROJECT/GLL3_640/GLL3_640.HTM

Similar PROJECT files (likely identical, not always AR_SEF) can be found in:
GO-J-PLS-4-SUMM-AVG-COUNTS-V1.0 / GO-J-PLS-4-SUMM-BROWSE-V1.0
GO-J-POS-6-SC-TRAJ-JUP-COORDS-V1.0 / GO-J-POS-6-MOON-TRAJ-JUP-COORDS-V1.0
GO-J-MAG-3-RDR-HIGHRES-V1.0 / GO-J-MAG-3-RDR-MAGSPHERIC-SURVEY-V1.0
[and likely other MAG volumes, and other fields/particle instruments]

Seems that **GO-J-PLS-3-RDR-FULLRES-V1.0**/DOCUMENT is the best collection as it has all PLS and PROJECT ones, including the AR_SEF orbit directories that are missing from GO-J-PLS-2-EDR-RAW-

TELEM-PACKETS-V1.0. Otherwise the files seem to be the same, bar some minor changes in the LBL files, between the two.
Also **GO-J-PLS-3-RDR-FULLRES-V1.0**/CALIB is the only Calibration directory in any current PLS dataset. Therefore the PDS volume **GO-J-PLS-3-RDR-FULLRES-V1.0** is the best one for PLS details.

## *Going through Galileo Documentation*

Two critical pages from: GO-J-PLS-2-EDR-RAW-TELEM-PACKETS-V1.0/DOCUMENT/PROJECT/GLL3_280/3280_P2A.PDF



A2.4 AACS POSITION AND RATE DATA

The AACS shall provide pointing vector and rate data. The pointing vector information shall be provided in the Earth Mean Equator (EME) 1950.0 coordinate system, the Ecliptic (ECL) 1950.0 coordinate system, and spacecraft relative coordinate system. The data packet schematic is shown in Figure A2.4.1 and described further in Table A2.4.1.

The AACS P&R data is encoded into 3 separately sized data packages for inclusion in four TDM Telemetry Formats. These inclusions are as indicated in Figure A2.4.1 and are described below.

- LPW & LNR: the full 12 word (192 bits) packet
- LPU : the first 6 words (96 bits) of the packet
- BPT : the 4th & 5th words (32 bits) of the packet

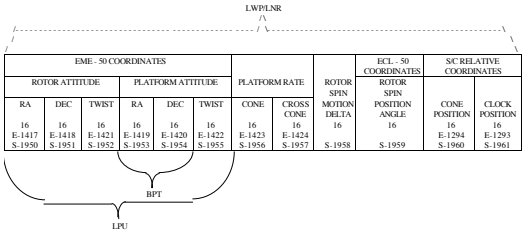


Figure A2.4.1. AACS Position and Rate Data



Table A2.4.1. AACS Position and Rate Data

| Data Description | Bits Frame | Data Start | Comments(1) |
|---|---|---|---|
| Rotor Attitude (2) | | | The Least Significant Bit (LSB) |
| Right Ascension (RA) | 16 | 0 | represents $1/2^{16}$ revolution. |
| Declination (DEC) | 16 | 16 | |
| Twist (3) | 16 | 32 | |
| | | | |
| Platform Attitude (2) | | | The Least Significant Bit (LSB) |
| Right Ascension (RA) | 16 | 48 | represents $1/2^{16}$ revolution. |
| Declination (DEC) | 16 | 64 | |
| Twist (4) | 16 | 80 | |
| | | | |
| Platform Rate | | | The LSB represents $1/2^{24}$ revolution |
| Cone | 16 | 96 | during 8-1/3 millisecond interval. |
| Cross Cone | 16 | 112 | |
| | | | |
| Rotor Spin Motion Delta | 16 | 128 | The LSB represents $1/2^{24}$ revolution during 8-1/3 millisecond interval. |
| Rotor Spin Position Angle (2,5) | 16 | 144 | The LSB represents $1/2^{24}$ revolution |
| Cone Position (2,6) | 16 | 160 | The LSB represents $1/2^{24}$ revolution |
| Clock Position (2,7) | 16 | 176 | |

Notes:
(1) Data is a 16 bit 2's complement number.
(2) Data is predicted ahead to RTI 0.
(3) Rotor twist represents rotation about the spacecraft Z-axis. The twist angle shall be defined as the angle from the projection of the Earth's North Pole onto the X-Y plane to the Rotor -X-axis (positive rotation about the Z-axis provides a positive twist angle.)
(4) Platform twist represents rotation about the scan platform boresight (L-axis). The twist angle shall be defined as the angle from the projection of the Earth's North Pole onto the M-N plane to the scan platform -M-axis (positive rotation about the L-axis provides a positive twist angle.
(5) Spin position angle represents the angle from the projection of the North Ecliptic Pole vector on the X-Y plane to the -X-axis. Positive rotation about the Z-axis provides a positive spin position angle.
(6) Cone position represents the null offset corrected encoder angle between the -Z-axis and the scan platform boresight (L-axis). An increasing encoder reading represents an increasing +N rotation of the scan platform with respect to the stator.
(7) Clock position represents the null offset corrected angle between the -Y-axis of the rotor and the SAS shaft (-N-axis, nominally the -Y-axis of the stator). An increasing encoder reading represents an increasing -Z rotation of the rotor with respect to the stator.

From above:
"(3) Rotor twist represents rotation about the spacecraft Z-axis. The twist angle shall be defined as the angle from the projection of the Earth's North Pole onto the X-Y plane to the Rotor -X-axis (positive rotation about the Z-axis provides a positive twist angle.)"
And:
"(5) Spin position angle represents the angle from the projection of the North Ecliptic Pole vector on the X-Y plane to the -X-axis. Positive rotation about the Z-axis provides a positive spin position angle."

This implies Rotor twist is from EME50, while Spin is from ECL50.
(Supports earlier MAG definition.)

Same document defines PLS telemetry in section A2.9, pages 187 to 205
"A2.9 PLASMA SUBSYSTEM TELEMETRY
This paragraph describes the format and content of the PLS output."

Within that is
“A2.9.4.3 Sector Sequencing Block. The Sector Sequencing Block consists of 8 bytes of data. Five of those determine the sector sequencing for the spin it is in, and subsequent spins until it is updated, or a new PLS packet starts. The contents of this block are shown in Figure A2.9.5.

| | |
|---|---|
| Byte 1 | Block I.D. (28=A, 2A=B, HEX) |
| Byte 2 | Block Size (6) |
| Byte 3 | AACS Clock angle of start of first sector ( 0 to 360 degrees, see A2.4, AACS Position and Rate Date) |
| Byte 4 | Duration of each energy (or mass) step, in 8.33 ms units |
| Byte 5 | Number of steps to be scanned in this sector |
| Byte 6 | Clock angle increment to start of next sector |
| Byte 7 | Number of sectors to be sampled in one spin |
| Byte 8 | End Code (FF HEX) |

Figure A2.9.5. Sector Sequencing Blocks

“Clock angle” is the phrase repeatedly used, even the PLS FMT file for level 3 data states:
SECTOR_ID: "AACS sector (clock angle) at start of spin-sector (0-255)."

## 8.4 AACS POSITION AND RATE DATA

The AACS Position and Rate data record is designed to a RIM cycle containing 91 minor frames. Each minor frame corresponds to a MOD91 count. The AACS record shall be placed onto each Science EDR as well as the Engineering EDR in time order. The logical record structure is diagrammed in Figure 8-2.

Processing Start/Stop
Refer to Subsection 8.2.

Record Buildup
AACS record buildup shall proceed with the extraction from the appropriate bit locations from minor frames 1 through 91 of each RIM cycle. Subsection 8.2 defines the basic data extraction procedure.

Record Header
The AACS record shall receive a standard record header (refer to Section 10).

Record Subheader
The AACS record shall not receive a subheader.

Data Block
The AACS data block contains data extracted from bits 3200 through bits 3391 of each of the 91 minor frames of a RIM cycle from the golay compressed LRS data block of the input SDR record. Specified word locations shall be maintained within the data block. Refer to Figure 8-3 for data block format and GLL-3-280 Appendix A for detailed definitions.

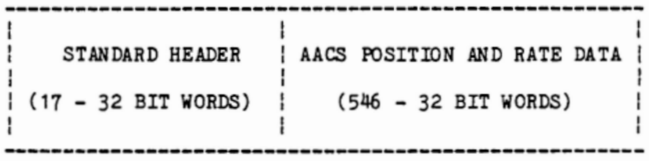


Figure 8-2. AACS Record

| EDR WORD | BITS 0 – 15 | 16 – 31 | 0 – 15 | 16 – 31 |
|---|---|---|---|---|
| 0 | ROTOR ATTITUDE RA (MF-1) | ROTOR ATTITUDE DEC (MF-1) | ROTOR ATTITUDE TWIST (MF-1) | PLATFORM ATTITUDE RA (MF-1) |
| 2 | PLATFORM ATT. DEC (MF-1) | PLATFORM ATT. TWIST (MF-1) | PLATFORM RATE CONE (MF-1) | PLATFORM RATE CROSS CONE (MF-1) |
| 4 | ROTOR SPIN MOTION DELTA (MF-1) | ROTOR SPIN POSITION ANGLE (MF-1) | S/C RELATIVE CONE (MF-1) | S/C RELATIVE CLOCK (MF-1) |
| | THE ABOVE STRUCTURE IS REPEATED 90 MORE TIMES TO COMPLETE THE RECORD OF 546 32-BIT WORDS | | | |
| 544 | | | | |

Figure 8-3. AACS Data Block Format

From: GO-J-PLS-3-RDR-FULLRES-V1.0/DOCUMENT/PROJECT/GLL3_180

File PAGE36.PNG:

3.7.6.3 Earth Mean Equator and Equinox, Epoch of 1950 (EME50) Coordinate System. This is an inertial coordinate system with its origin at the center of the earth and its axis constructed as follows: The Xe - axis is defined by a unit vector directed from the origin towards the Vernal Equinox at Epoch of 1950 and refers to the beginning of the Besselian year and corresponds to the Julian Ephemeris date 24 33282.423357. The Ye-axis lies on the earth mean equatorial plane with the positive direction defined at 90° clockwise rotation about the Xe - axis when looking towards the celestial north pole. The Ze - axis completes a right handed orthogonal coordinate system. In cartesian coordinates, an object's position is defined by its x, y, and z values.

In the EME 50 coordinate system using polar coordinates, the reference plane is the plane of the earth's mean equator which intersects the celestial sphere to give the celestial equator. (See Figure 11.) All great circles perpendicular to the celestial equator are called 'hour circles'; they pass through the north pole P and south pole Q of the heavens. See Figure 12 for a pictorial definition of this coordinate system. The origin for measuring the right ascension angle $\alpha$ is the vernal point (for the EME 50, this origin is the Vernal Equinox at Epoch of 1950 as defined above). The right ascension angel $\alpha$ is defined as the angle between the vernal point and the point of intersection of the hour circle of the object with the celestial equator. It is measured clockwise when looking at the north pole, and its value is given in hours, minutes, and seconds. The other coordinate, the declination $\delta$, is measured from the celestial equator along the hour circle of the object; it has a positive value from 0 to 90 deg in the direction of the celestial north pole, and negative in the direction of the south pole.

3.7.6.4 Ecliptic Epoch of 1950 (ECL50) Coordinate System. The plane of the ecliptic is chosen as the primary reference plane of this coordinate system. (See Figure 13.) As the origin for one coordinate, the ecliptic longitude $\lambda$, the vernal point for the Epoch of 1950 is chosen and refers to the beginning of the Besselian year and corresponds to the Julian Ephemeris date 24 33282.423357. The ecliptic longitude is measured from it (in the same direction as the apparent annual solar motion) to the point of intersection of the longitude circle of the object with the ecliptic. The longitude circles, or closures are the great circles perpendicular to the ecliptic and, therefore, passing through the poles of the ecliptic.

File PAGE37.PNG:

The values are stated in degrees from 0 to 360 deg with 0 starting at the vernal point and increasing in value clockwise when looking at the ecliptic north pole Ep. The other coordinate, the ecliptic latitude ß, is measured from the ecliptic along the closure of the celestial object in degrees, positive in the direction toward the ecliptic north pole and negative toward the south pole.

3.7.6.5 S/C Attitude Determination Coordinate System. This reference frame is an inertial coordinate system which is coincident with the rotor frame at the time at which Star #1 crosses the SS vertical (clock) slit. It is inertially fixed, and is updated each time Star #1 crosses the clock slit, until any external torque (thruster firing) is applied. Following the external torque, it is reinitialized when attitude determination resumes.

3.7.6.6 Scan Platform and Rotor Twist Angles. Platform twist is the angle from the projection of the 1950 North Celestial Pole onto the M-N plane to the -M axis measured in a right hand sense about the +L axis. Rotor twist is the angle from the projection of the 1950 North Celestial Pole onto the X-Y plane to the -X axis, measured in a right hand sense about the +Z axis.

Does not mention Spin, only Twist.

Section 3.7.2.1 states spun section (rotor) and despun section (stator), so PLS is on the Rotor.

## *Where is Galileo PLS mounted?*

From GO-J-PLS-3-RDR-FULLRES-V1.0/DOCUMENT/PROJECT/GLL3_180/PAGE69.PNG (which is document GLL-3-180C), section 4.4.6 states:

4.4.6 Plasma Subsystem (PLS) (ICD 10086756

The PLS instrument consists of a quadrispherical Lepedea plasma analyzer and is contained within a single package. The instrument has a FOV of 168 deg in cone and 12 deg in clock centered in the instrument aperture.

The configuration shall:

a. Provide for installation of the PLS on the spun section science boom such that an unobstructed FOV is attained while maximizing the distance to the RTG's consistent with other S/C requirements.

b. Provide mounting alignment accuracy within the requirements of GLL-3-170.

This figure is from a page in GLL-3-180C (stated at top right of page but cropped out here):
Noted on the figure is SC +X is up, +Y is right, and +Z is into the paper.
Also noted on the figure, CLCK is 0 degrees at -Y, and 270 degrees at +X.

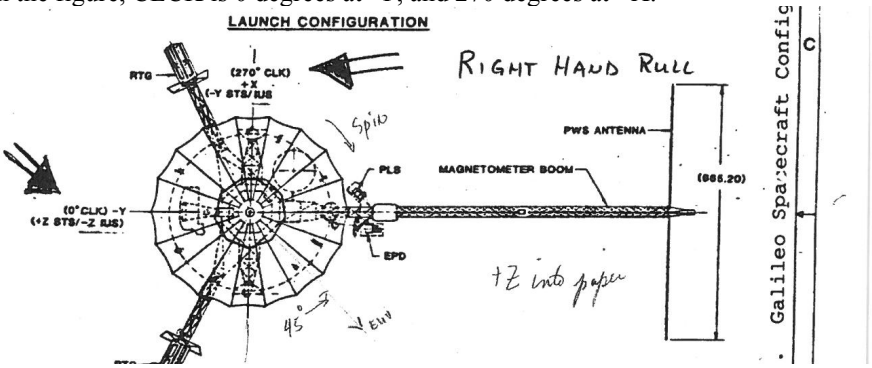


Note spin direction that is hand written is correct (opposite of PLS instrument paper).

A subsequent plot (presuming from same document) zooms in, and is further cropped here. Figure does note that now SC +Y is down, and +X is to the right – confirming above image.

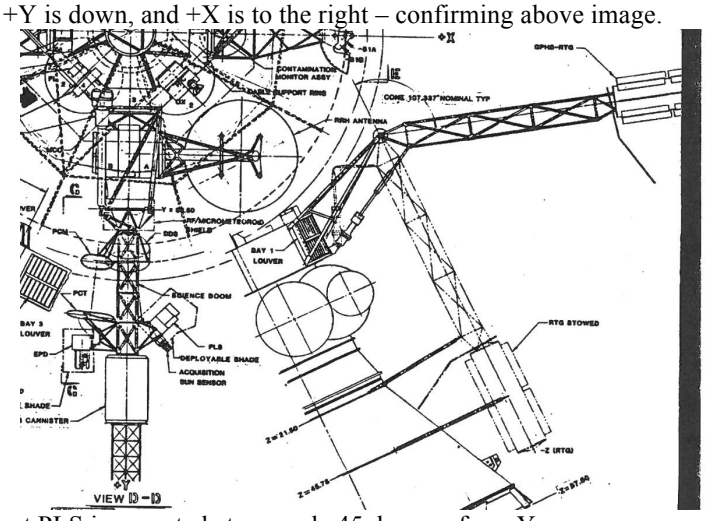


Both figures suggest PLS is mounted at an angle 45 degrees from Y.

**APPENDIX B: Comparing ROTOR Co-ordinates to SPICE output**

Although not utilized in this study – this is the comparison that was done to confirm and explain how rotor co-ordinates Right Ascension (RA), Declination (DEC), Spin and Twist could be used instead of SPICE. This is provided as a guide to aid anyone wishing to re-examine Galileo Data.

The PDS volume GO-J-POS-6-REDR-ROTOR-ATTITUDE-V1.0 contains the RA/DEC/SPIN and TWIST values throughout the Galileo mission. For this test we have loaded in file ROTATT01.TAB (from this PDS volume) to obtain RA and DEC and check the spin axis of the spacecraft matches that given by SPICE, using Matlab.

```
% MATLAB Code – assuming you've loaded in correct SPICE kernels
% and have et as single (scalar) ephemeris time
SC_ID   = -77      ; % Galileo
SC_Bus  = -77000   ; % Galileo Bus – best I can tell

% Calculate a tolerance for pointing data. Use 200 seconds,
% convert to ticks by multiplying by the number of ticks per second.
tol_sec = 200.0;  % Duration in seconds
% so number of ticks in that time is difference between time tol_sec
% and time zero.  We add 100 to both as equivalent IDL code does not
% work unless above more than the number of leap seconds to date.
toltik =  cspice_scencd(SC_ID, cspice_sce2s(SC_ID, tol_sec + 100)) ...
       - cspice_scencd(SC_ID, cspice_sce2s(SC_ID,    0    + 100));
% cspice_ckgpav requires encoded spacecraft clock time.
sclkdp = cspice_sce2c( SC_ID, et );
[cmat,av,clkout,found] = cspice_ckgpav(SC_Bus, sclkdp, toltik,'B1950');
% Definintion of cmat from the help of ckgpav
% cmat   rotation matrix(ces) that transform components of a vector
%        expressed in the frame specified by 'ref' to components
%        expressed in the frame tied to the instrument, spacecraft, or
%        other structure at time(s) 'clkout'.
% This array is 'B1950->spacecraft', transpose for 'spacecraft->B1950'
cTmat = cmat'; % Transpose (3x3 matrix) with the ' command
%if et was not scalar, cmat is size 3x3x{numel(et)}, then do this:
%cTmat = permute(cmat,[2, 1, 3]); % Transpose first 2 dimensions only
% Spin Vector (size 3x1) from SPICE is then:
spinSPICE = cTmat(1:3,3);  % for scalar et, this is the spin vector

% Spin Vector (size 3x1) from Rotor RA and DEC
% From Appendix A of Stone's thesis
% In this example, RA = 4.93433 rads, DEC = -0.43566 rads
spinROTOR = [ cos(RA).*cos(DEC) ; sin(RA)*cos(DEC); sin(DEC)];
```

If the `toltik` tolerance is not met, `cmat` is basically zero and the above fails, so only use when `found` = 1, or increase your tolerance until `found` = 1 for all.
For orbit 00, no values had a found = 1 with a tolerance of 200s.
For orbit 01, the first case where `found` equaled 1 was 461 records in (1996-06-23T16:02:21), and with the above code snippets we get:

```
spinROTOR = [ 0.1996 ; -0.8844 ; -0.4220]
spinSPICE = [ 0.1996 ; -0.8844 ; -0.4220]
```

Clearly these values agree.

## APPENDIX C: Quantization of Measured Counts Per Accumulation

| 1-byte look up value | Lower count/accum. | Upper count/accum. |
|---|---|---|
| 0 | 0 | 0 |
| 1 | 1 | 1 |
| 2 | 2 | 2 |
| 3 | 3 | 3 |
| 4 | 4 | 4 |
| 5 | 5 | 5 |
| 6 | 6 | 6 |
| 7 | 7 | 7 |
| 8 | 8 | 8 |
| 9 | 9 | 9 |
| 10 | 10 | 10 |
| 11 | 11 | 11 |
| 12 | 12 | 12 |
| 13 | 13 | 13 |
| 14 | 14 | 14 |
| 15 | 15 | 15 |
| 16 | 16 | 16 |
| 17 | 17 | 17 |
| 18 | 18 | 18 |
| 19 | 19 | 19 |
| 20 | 20 | 20 |
| 21 | 21 | 21 |
| 22 | 22 | 22 |
| 23 | 23 | 23 |
| 24 | 24 | 24 |
| 25 | 25 | 25 |
| 26 | 26 | 26 |
| 27 | 27 | 27 |
| 28 | 28 | 28 |
| 29 | 29 | 29 |
| 30 | 30 | 30 |
| 31 | 31 | 31 |
| 32 | 32 | 33 |
| 33 | 34 | 35 |
| 34 | 36 | 37 |
| 35 | 38 | 39 |
| 36 | 40 | 41 |
| 37 | 42 | 43 |
| 38 | 44 | 45 |
| 39 | 46 | 47 |
| 40 | 48 | 49 |
| 41 | 50 | 51 |
| 42 | 52 | 53 |
| 43 | 54 | 55 |
| 44 | 56 | 57 |
| 45 | 58 | 59 |
| 46 | 60 | 61 |
| 47 | 62 | 63 |
| 48 | 64 | 67 |
| 49 | 68 | 71 |
| 50 | 72 | 75 |
| 51 | 76 | 79 |
| 52 | 80 | 83 |
| 53 | 84 | 87 |
| 54 | 88 | 91 |
| 55 | 92 | 95 |
| 56 | 96 | 99 |
| 57 | 100 | 103 |
| 58 | 104 | 107 |
| 59 | 108 | 111 |
| 60 | 112 | 115 |
| 61 | 116 | 119 |
| 62 | 120 | 123 |
| 63 | 124 | 127 |
| 64 | 128 | 135 |
| 65 | 136 | 143 |
| 66 | 144 | 151 |
| 67 | 152 | 159 |
| 68 | 160 | 167 |
| 69 | 168 | 175 |
| 70 | 176 | 183 |
| 71 | 184 | 191 |
| 72 | 192 | 199 |
| 73 | 200 | 207 |
| 74 | 208 | 215 |
| 75 | 216 | 223 |
| 76 | 224 | 231 |
| 77 | 232 | 239 |
| 78 | 240 | 247 |
| 79 | 248 | 255 |
| 80 | 256 | 271 |
| 81 | 272 | 287 |
| 82 | 288 | 303 |
| 83 | 304 | 319 |
| 84 | 320 | 335 |
| 85 | 336 | 351 |
| 86 | 352 | 367 |
| 87 | 368 | 383 |
| 88 | 384 | 399 |
| 89 | 400 | 415 |
| 90 | 416 | 431 |
| 91 | 432 | 447 |
| 92 | 448 | 463 |
| 93 | 464 | 479 |
| 94 | 480 | 495 |
| 95 | 496 | 511 |
| 96 | 512 | 543 |
| 97 | 544 | 575 |
| 98 | 576 | 607 |
| 99 | 608 | 639 |
| 100 | 640 | 671 |
| 101 | 672 | 703 |
| 102 | 704 | 735 |
| 103 | 736 | 767 |
| 104 | 768 | 799 |
| 105 | 800 | 831 |
| 106 | 832 | 863 |
| 107 | 864 | 895 |

| | | |
|---|---|---|
| 108 | 896 | 927 |
| 109 | 928 | 959 |
| 110 | 960 | 991 |
| 111 | 992 | 1023 |
| 112 | 1024 | 1087 |
| 113 | 1088 | 1151 |
| 114 | 1152 | 1215 |
| 115 | 1216 | 1279 |
| 116 | 1280 | 1343 |
| 117 | 1344 | 1407 |
| 118 | 1408 | 1471 |
| 119 | 1472 | 1535 |
| 120 | 1536 | 1599 |
| 121 | 1600 | 1663 |
| 122 | 1664 | 1727 |
| 123 | 1728 | 1791 |
| 124 | 1792 | 1855 |
| 125 | 1856 | 1919 |
| 126 | 1920 | 1983 |
| 127 | 1984 | 2047 |
| 128 | 2048 | 2175 |
| 129 | 2176 | 2303 |
| 130 | 2304 | 2431 |
| 131 | 2432 | 2559 |
| 132 | 2560 | 2687 |
| 133 | 2688 | 2815 |
| 134 | 2816 | 2943 |
| 135 | 2944 | 3071 |
| 136 | 3072 | 3199 |
| 137 | 3200 | 3327 |
| 138 | 3328 | 3455 |
| 139 | 3456 | 3583 |
| 140 | 3584 | 3711 |
| 141 | 3712 | 3839 |
| 142 | 3840 | 3967 |
| 143 | 3968 | 4095 |
| 144 | 4096 | 4351 |
| 145 | 4352 | 4607 |
| 146 | 4608 | 4863 |
| 147 | 4864 | 5119 |
| 148 | 5120 | 5375 |
| 149 | 5376 | 5631 |
| 150 | 5632 | 5887 |
| 151 | 5888 | 6143 |
| 152 | 6144 | 6399 |
| 153 | 6400 | 6655 |
| 154 | 6656 | 6911 |
| 155 | 6912 | 7167 |
| 156 | 7168 | 7423 |
| 157 | 7424 | 7679 |
| 158 | 7680 | 7935 |
| 159 | 7936 | 8191 |
| 160 | 8192 | 8703 |
| 161 | 8704 | 9215 |
| 162 | 9216 | 9727 |
| 163 | 9728 | 10239 |
| 164 | 10240 | 10751 |
| 165 | 10752 | 11263 |
| 166 | 11264 | 11775 |
| 167 | 11776 | 12287 |
| 168 | 12288 | 12799 |
| 169 | 12800 | 13311 |
| 170 | 13312 | 13823 |
| 171 | 13824 | 14335 |
| 172 | 14336 | 14847 |
| 173 | 14848 | 15359 |
| 174 | 15360 | 15871 |
| 175 | 15872 | 16383 |
| 176 | 16384 | 17407 |
| 177 | 17408 | 18431 |
| 178 | 18432 | 19455 |
| 179 | 19456 | 20479 |
| 180 | 20480 | 21503 |
| 181 | 21504 | 22527 |
| 182 | 22528 | 23551 |
| 183 | 23552 | 24575 |
| 184 | 24576 | 25599 |
| 185 | 25600 | 26623 |
| 186 | 26624 | 27647 |
| 187 | 27648 | 28671 |
| 188 | 28672 | 29695 |
| 189 | 29696 | 30719 |
| 190 | 30720 | 31743 |
| 191 | 31744 | 32767 |
| 192 | 32768 | 34815 |
| 193 | 34816 | 36863 |
| 194 | 36864 | 38911 |
| 195 | 38912 | 40959 |
| 196 | 40960 | 43007 |
| 197 | 43008 | 45055 |
| 198 | 45056 | 47103 |
| 199 | 47104 | 49151 |
| 200 | 49152 | 51199 |
| 201 | 51200 | 53247 |
| 202 | 53248 | 55295 |
| 203 | 55296 | 57343 |
| 204 | 57344 | 59391 |
| 205 | 59392 | 61439 |
| 206 | 61440 | 63487 |
| 207 | 63488 | 65535 |
| 208 | 65536 | 69631 |
| 209 | 69632 | 73727 |
| 210 | 73728 | 77823 |
| 211 | 77824 | 81919 |
| 212 | 81920 | 86015 |
| 213 | 86016 | 90111 |
| 214 | 90112 | 94207 |
| 215 | 94208 | 98303 |
| 216 | 98304 | 102399 |
| 217 | 102400 | 106495 |
| 218 | 106496 | 110591 |
| 219 | 110592 | 114687 |
| 220 | 114688 | 118783 |
| 221 | 118784 | 122879 |
| 222 | 122880 | 126975 |
| 223 | 126976 | 131071 |

**References**

Bevington, P. R., and D. K. Robinson (2003), Data Reduction and Error Analysis for the Physical Sciences, 3rd ed., McGraw-Hill, Univ. of California.

Delamere, P.A., F. Bagenal, A. Steffl (2005), Radial variations in the Io plasma torus during the Cassini era. *J. Geophys. Res. 110,* A12223.

Frank, L. A., K. L. Ackerson, J. A. Lee, M. R. English and G. L. Pickett (1992), The Plasma Instrumentation for the Galileo Mission, *Sp. Sci. Rev., 60,* 283-307

Wilson, R. J. (2015), Error analysis for numerical estimates of space plasma parameters, *Earth and Space Science, 2,* 201–222. doi:10.1002/2014EA000090.